

1     **Assessing the impact of stratospheric aerosol injection**  
2             **on U.S. convective weather environments**

3             **Ivy Glade<sup>1</sup>, James W. Hurrell<sup>1</sup>, Lantao Sun<sup>1</sup>, Kristen L. Rasmussen<sup>1</sup>**

4             <sup>1</sup>Department of Atmospheric Science, Colorado State University, Fort Collins, CO, USA

5     **Key Points:**

- 6             • SAI may prevent future increases in the magnitude of thermodynamic parameters  
7                 relevant to the formation of severe weather over the U.S.
- 8             • Future changes in wind shear, a kinematic parameter, is driven largely by changes  
9                 in tropical precipitation whether or not SAI is deployed.
- 10            • Internal decadal-scale climate variability is likely to impact future projections of  
11                 regional changes in convective weather environments.

---

Corresponding author: Ivy Glade, [ivyglade@rams.colostate.edu](mailto:ivyglade@rams.colostate.edu)

**Abstract**

Continued climate warming, together with the overall evaluation and implementation of a range of climate mitigation and adaptation approaches, has prompted increasing research into proposed solar climate intervention (SCI) methods, such as stratospheric aerosol injection (SAI). SAI would use aerosols to reflect a small amount of incoming solar radiation away from Earth to stabilize or reduce future warming due to increasing greenhouse gas concentrations. Research into the possible risks and benefits of SAI relative to the risks from climate change is emerging. There is not yet, however, an adequate understanding of how SAI might impact human and natural systems. For instance, little to no research to date has examined how SAI might impact environmental conditions critical to the formation of severe convective weather over the United States (U.S.). This study uses ensembles of Earth system model simulations of future climate change, with and without hypothetical SAI deployment, to examine possible future changes in thermodynamic and kinematic parameters critical to the formation of severe weather during convectively active seasons over the U.S. Results show that simulated forced changes in thermodynamic parameters are significantly reduced under SAI relative to a no-SAI world, while simulated changes in kinematic parameters are more difficult to distinguish. Also, unforced internal climate variability is likely to significantly modulate the projected forced climate changes over large regions of the U.S.

**1 Introduction**

Global carbon dioxide (CO<sub>2</sub>) emissions have increased every decade since the 1960s and are projected to continue to increase over at least the next several decades (Friedlingstein et al., 2022; Jiang & Guan, 2016; Peters et al., 2012). It is therefore very unlikely that global climate warming will be limited to 1.5 or even 2°C above pre-industrial temperatures unless action is taken soon to drastically reduce emissions (IPCC, 2021). In fact, climate warming is projected to be over 2°C by the end of the century under moderate and current policy-relevant emissions scenarios, surpassing what is considered to be a safe threshold of warming (IPCC, 2021; Riahi et al., 2017; UNEP, 2022). Climate impacts such as drought intensification (Mukherjee et al., 2018; Strzepek et al., 2010), increases in extreme precipitation (M. R. Allen & Ingram, 2002; Donat et al., 2016; Dougherty & Rasmussen, 2020; Prein et al., 2017) and continued sea ice loss (Stroeve et al., 2012) are projected to worsen over the coming decades (IPCC, 2021). Future changes

44 also include the potential for increases in the frequency and intensity of severe convective  
45 weather over large portions of the United States (U.S.) (Diffenbaugh et al., 2013;  
46 Hoogewind et al., 2017; Lepore et al., 2021; K. L. Rasmussen et al., 2017; Seeley &  
47 Romps, 2015; Tippet et al., 2015; Trapp et al., 2007, 2009, 2019).

48 Given slow progress toward reducing fossil fuel emissions and the urgency to limit  
49 continued temperature warming, the U.S. National Academies of Science, Engineering and  
50 Medicine (NASEM) recently recommended the formation of a transdisciplinary research  
51 program to identify the potential benefits and risks of solar climate intervention (SCI)  
52 relative to the risks posed by climate change (NASEM, 2021). Most SCI approaches  
53 would cool the planet by reflecting a small amount of incoming solar radiation away from  
54 Earth, potentially minimizing some of the worst consequences of anthropogenic climate  
55 change while buying more time for mitigation and the deployment of CO<sub>2</sub> removal  
56 technologies. Stratospheric aerosol injection (SAI) is one proposed form of SCI that would  
57 involve, perhaps, the injection of sulfur dioxide (SO<sub>2</sub>) into the stratosphere, which would  
58 react with hydrogen and oxygen to form highly reflective sulfate aerosols (Crutzen, 2006;  
59 Rasch et al., 2008; Richter et al., 2022).

60 Several Earth-system models have been used to simulate a future climate with SAI under  
61 different climate change scenarios (Kravitz et al., 2011; Richter et al., 2022; Tilmes et al.,  
62 2018; Vioni et al., 2023). Research to date has included examining changes in global and  
63 regional temperature and precipitation (Hueholt et al., 2023; Richter et al., 2022; Tilmes  
64 et al., 2018), atmospheric circulation patterns (Bednarz et al., 2022), extreme temperature  
65 and precipitation events (Barnes et al., 2022; Ji et al., 2018), and ecological responses  
66 (Zarnetske et al., 2021), in addition to potential deployment technologies (Lockley et al.,  
67 2022; Smith & Wagner, 2018). Such studies have demonstrated that SAI could potentially  
68 be deployed to stabilize or reduce global mean temperature to a specific temperature  
69 target (Richter et al., 2022; Tilmes et al., 2018; Vioni et al., 2021); however, research has  
70 also indicated that regional impacts of SAI could be both positive and negative. For  
71 example, major African river basins may have enhanced drought risk because SAI is  
72 projected to cause precipitation decreases that overcompensate for projected increases due  
73 to climate warming (Abiodun et al., 2021). On the other hand, future projections indicate  
74 that SAI has the potential to reduce Greenland ice sheet mass loss (Moore et al., 2019)  
75 and minimize the loss of Arctic sea ice (Lee et al., 2023).

76 While research on the potential impacts of SAI has been increasing and broadening in  
77 recent years, current research remains scattered and ad hoc, so a holistic understanding of  
78 how SAI would impact Earth and human systems is limited (NASEM, 2021). For  
79 instance, while there have been studies documenting the impact of climate change on the  
80 large-scale environments in which severe weather (as defined by Galway, 1989) forms  
81 (Diffenbaugh et al., 2013; Franke et al., 2023; Hoogewind et al., 2017; Lepore et al., 2021;  
82 K. L. Rasmussen et al., 2017; Seeley & Romps, 2015; Trapp et al., 2007, 2009; Chen et al.,  
83 2020), there are no studies that have examined the potential impact of SAI on those  
84 environments. The topic is of relevance given increasing economic impacts and more  
85 frequent billion dollar U.S. severe weather disasters in recent decades (NCEI, 2022).

86 Large-scale parameters and proxies have been used to identify what environmental  
87 conditions are favorable to the formation of severe weather, largely in order to improve  
88 short-term predictability and overcome discontinuities and inconsistencies in limited  
89 observational records (e.g., Doswell et al., 1996; E. N. Rasmussen & Blanchard, 1998;  
90 Brooks et al., 2003; Craven & Brooks, 2004). More recently, such parameters and proxies  
91 have also been used to predict how the behavior of severe weather might change on longer  
92 time scales, such as through the end of the century (e.g., Diffenbaugh et al., 2013; Franke  
93 et al., 2023; Hoogewind et al., 2017; Lepore et al., 2021; K. L. Rasmussen et al., 2017;  
94 Trapp et al., 2007). In part, this is because integrating convection-permitting models over  
95 long periods of time is computationally expensive, and these parameters and proxies are  
96 resolvable using coarser resolution Earth-system models.

97 Parameters commonly analyzed include convective available potential energy (CAPE),  
98 convective inhibition (CIN), and the wind shear from the surface to  $\sim 6$  km (S06). With  
99 climate change, the magnitudes of both CAPE and CIN are projected to increase in the  
100 U.S. east of the Rocky Mountains in both the spring and summer (Diffenbaugh et al.,  
101 2013; Franke et al., 2023; Hoogewind et al., 2017; Lepore et al., 2021; K. L. Rasmussen et  
102 al., 2017; Trapp et al., 2007; Chen et al., 2020). Increases in the magnitude of CAPE and  
103 CIN have been attributed to increases in temperature and moisture throughout the  
104 troposphere (K. L. Rasmussen et al., 2017, see also Fig. S2) and decreases in low-level  
105 relative humidity (Chen et al., 2020). Wind shear (S06) is also generally projected to  
106 decrease in both the spring and summer seasons across the U.S., especially east of the  
107 Rockies (Trapp et al., 2007; Hoogewind et al., 2017; Lepore et al., 2021), a change that

108 largely reflects decreases in the zonal wind at  $\sim 6$  km (Diftenbaugh et al., 2013; Franke et  
109 al., 2023).

110 Combined proxies that consider the integrated effects of more than one convective  
111 weather environment parameter have also been analyzed (Diftenbaugh et al., 2013;  
112 Hoogewind et al., 2017; Lepore et al., 2021; Seeley & Romps, 2015; Trapp et al., 2007,  
113 2009). Proxies that consider both the thermodynamic and kinematic characteristics of the  
114 environments have been shown to better discriminate between environments conducive to  
115 ordinary thunderstorms, supercells, and tornadic supercells than individual  
116 thermodynamic or kinematic parameters alone (E. N. Rasmussen & Blanchard, 1998).  
117 CAPES06, defined as the product of CAPE and S06, has been used to distinguish  
118 significant severe storms from those that are less severe (Brooks et al., 2003;  
119 E. N. Rasmussen & Blanchard, 1998). This proxy is often used in tandem with other  
120 convective weather environment parameters to describe whether an environment is  
121 favorable to the formation of severe weather on a given day (Diftenbaugh et al., 2013;  
122 Hoogewind et al., 2017; Lepore et al., 2021; Seeley & Romps, 2015; Trapp et al., 2007).  
123 The number of days with high magnitude CAPES06 are projected to increase with future  
124 warming across the eastern U.S. (Seeley & Romps, 2015). Diftenbaugh et al. (2013)  
125 suggests that CAPES06 is expected to increase across the eastern U.S. even though S06 is  
126 projected to decrease, because decreases in S06 are expected to occur on days when  
127 CAPE is already low.

128 Previous research examining projections of convective weather environments has mostly  
129 considered high emissions trajectories that are not consistent with current climate  
130 policies. In this study, the potential impact of climate warming on convective weather  
131 environments in the U.S. is examined using a 10-member ensemble of Earth-system model  
132 simulations under the Shared Socioeconomic Pathway 2-4.5 (SSP2-4.5) emissions scenario.  
133 This is a “middle of the road” scenario more consistent with current climate policies. It  
134 projects  $\sim 2.7^\circ\text{C}$  of global warming by the end of the century (O’Neill et al., 2017) and  
135 considers the slow development and deployment of sustainability practices such as  $\text{CO}_2$   
136 emissions reduction and removal technologies (IPCC, 2021; Riahi et al., 2017). In  
137 addition, parallel climate change integrations with a hypothetical SAI deployment are  
138 analyzed to document the potential impact of SAI on large-scale convective weather  
139 environments, relative to the impacts from climate change alone. To our knowledge, this

140 is the first study to examine the potential influence of SAI on future convective weather  
141 environments.

## 142 **2 Methodology**

### 143 **2.1 Model Information**

144 This study utilizes a set of parallel simulations of climate change with and without SAI;  
145 specifically, the Assessing Responses and Impacts of Solar climate intervention on the  
146 Earth system using stratospheric aerosol injection (ARISE-SAI; Richter et al., 2022).  
147 These simulations were performed using the freely available Community Earth System  
148 Model version 2 (CESM2), a fully coupled model with the Whole Atmosphere Community  
149 Climate Model version 6 (WACCM6) as the atmospheric component (Danabasoglu et al.,  
150 2020; Gettelman et al., 2019). WACCM6 is a high-top model with a well-represented  
151 stratosphere that includes 70 vertical levels with a model top of  $4.5 \times 10^{-6}$  hPa ( $\sim 130$  km)  
152 and a horizontal resolution of  $1.25^\circ$  longitude and  $0.9^\circ$  latitude (Danabasoglu et al.,  
153 2020). ARISE-SAI consists of two 10-member ensembles of climate change with and  
154 without SAI. Both ensembles follow the moderate SSP2-4.5 emissions scenario (O'Neill et  
155 al., 2017). The ARISE-SAI climate change simulations consist of five members that run  
156 from 2015-2100 and were carried out as a part of the Coupled Model Intercomparison  
157 Project Phase 6 (Eyring et al., 2016). Five other ensemble members cover the period from  
158 2015-2069 and were branched off from three existing historical CESM2-WACCM6  
159 simulations (1850-2014) with the addition of a small temperature perturbation at the first  
160 model time step (Richter et al., 2022).

161 The first five members of the ensemble with a hypothetical SAI deployment were  
162 initialized in 2035 using the first five members of the climate change (SSP2-4.5) ensemble.  
163 The last five members were initialized in a similar way, but with the addition of a small  
164 temperature perturbation (Richter et al., 2022). Each of the 10 SAI simulations extend  
165 through 2069, with  $\text{SO}_2$  being injected into the stratosphere continuously beginning in  
166 2035 in order to maintain global mean temperature at  $\sim 1.5^\circ\text{C}$  above its pre-industrial  
167 value. In addition, the ARISE-SAI injection strategy is designed to maintain the  
168 equator-to-pole and interhemispheric temperature gradients to values consistent with  
169 those observed at the  $1.5^\circ\text{C}$  temperature target (Kravitz et al., 2017; MacMartin et al.,  
170 2014; Richter et al., 2022). The stabilizing influence of SAI is clear when examining not

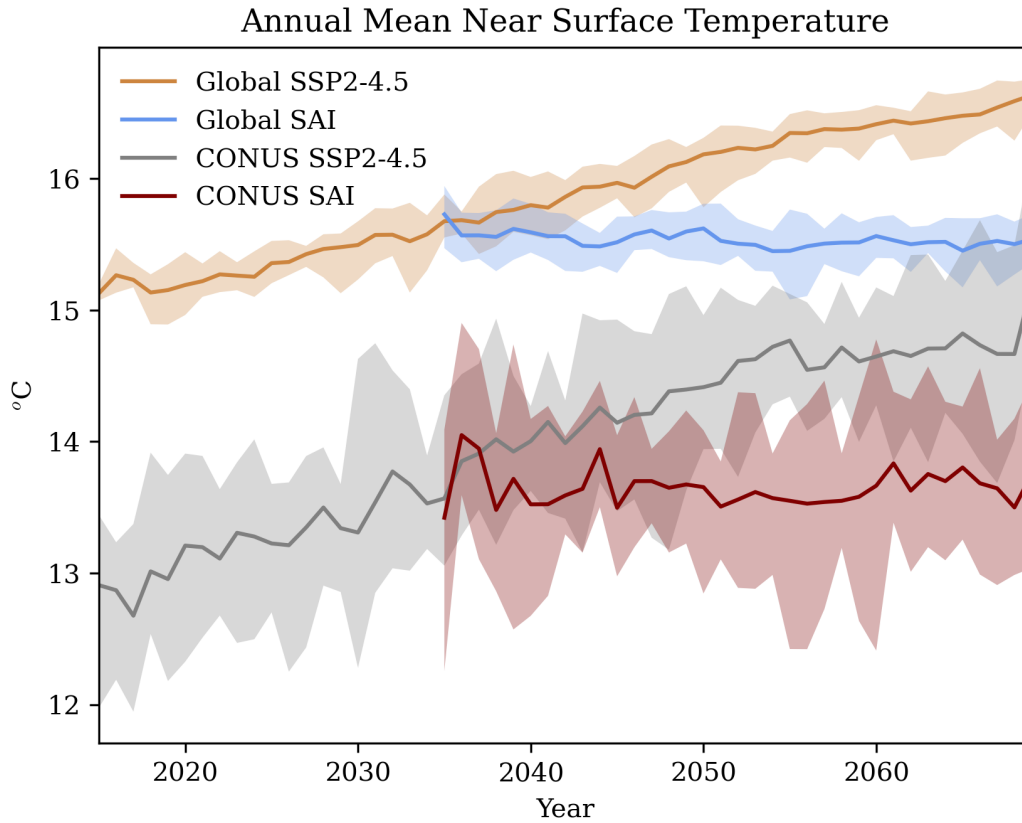


Figure 1: Annual mean near-surface (2 m) temperature from the SSP2-4.5 simulations (2015-2069) and the simulations where SAI is deployed (2035-2069). Results averaged over the globe are given by the tan (SSP2-4.5) and blue (SAI) lines, while those averaged over the contiguous U.S. are given by the gray (SSP2-4.5) and red (SAI) lines. Ensemble means are shown by the thick solid lines, while the minimum and maximum ranges of the individual ensemble members are shown by the corresponding color shading.

171 only the time series of global 2 m temperature change (Hueholt et al., 2023; Richter et al.,  
 172 2022), but also that for the contiguous U.S (CONUS) (Figure 1).

## 173 **2.2 Convective Weather Environment Parameters and Proxies**

174 CAPE ( $\text{J kg}^{-1}$ ) and CIN ( $\text{J kg}^{-1}$ ) are thermodynamic parameters which consider the  
 175 temperature and moisture content of the atmosphere (Doswell & Rasmussen, 1994).  
 176 CAPE is a measure of potential energy that is defined by the vertical integral of buoyancy  
 177 from the level of free convection to the equilibrium level, and is analogous to updraft

178 velocity (Doswell & Rasmussen, 1994; E. N. Rasmussen & Blanchard, 1998; Trapp et al.,  
179 2007). CIN represents the negative buoyancy and is indicative of the potential to suppress  
180 convective motions (E. N. Rasmussen & Blanchard, 1998). CAPE and CIN were  
181 calculated as the most-unstable parcel in the lowest 3000 m of the atmosphere (MUCAPE  
182 and MUCIN), which is a useful method for capturing cases of elevated instability, while  
183 being effective at identifying low-level or surface-based instability when present (Doswell  
184 & Rasmussen, 1994).

185 S06 ( $\text{m s}^{-1}$ ) is a kinematic parameter that is representative of the change in the  
186 horizontal wind vector from  $\sim 10$  m above ground-level to approximately 6 km altitude.  
187 This measure of wind shear is used to diagnose whether or not an environment is  
188 favorable to the formation of significant severe thunderstorms (Brooks et al., 2003;  
189 E. N. Rasmussen & Blanchard, 1998). In particular, small magnitudes of S06 are typically  
190 associated with the development of relatively small, short-lived single-cell thunderstorms,  
191 while larger magnitudes of S06 are typically associated with the potential for development  
192 of supercell thunderstorms, which are longer-lived, more organized, and more intense  
193 (Weisman & Klemp, 1982).

194 The combination of CAPE and 0-6 km wind shear (CAPES06;  $\text{m}^3 \text{s}^{-3}$ ) is a good  
195 discriminator for significant severe thunderstorm events (Brooks et al., 2003; Marsh et al.,  
196 2007; E. N. Rasmussen & Blanchard, 1998; Trapp et al., 2007). CAPES06 is considered  
197 simply as the product of CAPE and S06. Some previous studies have weighted S06 more  
198 heavily than CAPE (Brooks et al., 2003; Seeley & Romps, 2015), but Seeley and Romps  
199 (2015) note that varying the weight of S06 in calculations of CAPES06 did not have a  
200 large impact on future projections of favorable convective weather environments.

201 While results are presented as spatial maps over the CONUS, area-averaged statistics over  
202 the Southeast and Midwest regions are also computed. The Southeast is defined as the  
203 grid points bounded by  $39^\circ$ - $48^\circ$ N and  $255^\circ$ - $274^\circ$ W, while the Midwest is defined as the  
204 region within  $30^\circ$ - $39^\circ$ N and  $255^\circ$ - $280^\circ$ W (Figure S1). While all seasons and other regions  
205 over the U.S. were examined, the analysis here is restricted to the Southeast region during  
206 the boreal spring season (MAM) and the Midwest region during the boreal summer  
207 season (JJA). These regions and seasons were chosen subjectively based on the  
208 climatological seasonal distributions of both convective weather environments and severe  
209 weather events (e.g., Kelly et al., 1985; Doswell et al., 2005; Brooks et al., 2007; Taszarek

210 et al., 2020). The representation of convective weather environments in both the  
211 Community Atmosphere Model version 6 (CAM6) (Danabasoglu et al., 2020), an  
212 atmosphere only model, and CESM2-CAM6, a fully coupled Earth-system model, have  
213 been validated against the fifth generation of the high resolution global reanalysis dataset  
214 produced by ECMWF (ERA5) (Franke et al., 2023; Li et al., 2020; Chen et al., 2020).  
215 CAM6 is the low-top version of WACCM6, where the two models have the same vertical  
216 structure up to 87 hPa and nearly identical parameterizations (Danabasoglu et al., 2020).  
217 These validations have shown that both CAM6 and CESM2-CAM6 are able to well  
218 represent convective weather environments over the eastern CONUS, as well as the  
219 synoptic features (Li et al., 2020) and the influence of large-scale modes of variability,  
220 such as the El Niño Southern Oscillation (ENSO; Franke et al., 2023).

221 Most previous studies that have considered convective weather environment parameters  
222 have calculated these indices using model output at 00 Z, which is known to represent the  
223 time when MUCAPE is maximized in the central to eastern U.S. (e.g., Trapp et al., 2007;  
224 Diffenbaugh et al., 2013; Seeley & Romps, 2015). However, only daily mean data are  
225 available for all 10 of the ARISE-SAI ensemble members. To assess the suitability of using  
226 daily averaged data, 00 Z data were extracted from one ensemble member from the  
227 CESM2 Large Ensemble (CESM2-LE; Rodgers et al., 2021) and results were compared to  
228 those computed from the daily averaged data from the same simulation. The CESM2-LE  
229 is a 100-member ensemble that runs from 1850-2100 and follows the SSP3-7.0 emissions  
230 scenario, which warms more and has slower development of mitigation and adaptation  
231 practices relative to SSP2-4.5 (O'Neill et al., 2017). The CESM2-LE utilizes the low-top  
232 atmospheric component of CESM2 (CAM6; Rodgers et al., 2021).

233 The time evolutions from 2015-2069 of MUCAPE, MUCIN, S06, and CAPES06 computed  
234 at 00 Z were compared to those computed as a daily mean quantity. The analysis was  
235 based on anomalies relative to 2015-2034 climatologies. The time evolution of CAPES06  
236 anomalies for the Southeast in MAM and the Midwest in JJA indicates high correlation  
237 between the sub-daily and daily mean anomalies in both regions ( $r = 0.988$  and  $r =$   
238  $0.946$ ) (Figure 2). Correlations between sub-daily and daily mean anomalies are similarly  
239 high for MUCAPE, MUCIN and S06 (not shown). Thus, while differences exist in the  
240 absolute magnitude of the convective weather environment parameters when computed  
241 from sub-daily relative to daily mean data (especially for MUCIN, which is maximized at  
242 night rather than in the afternoon due to nocturnal stability in the boundary layer), the

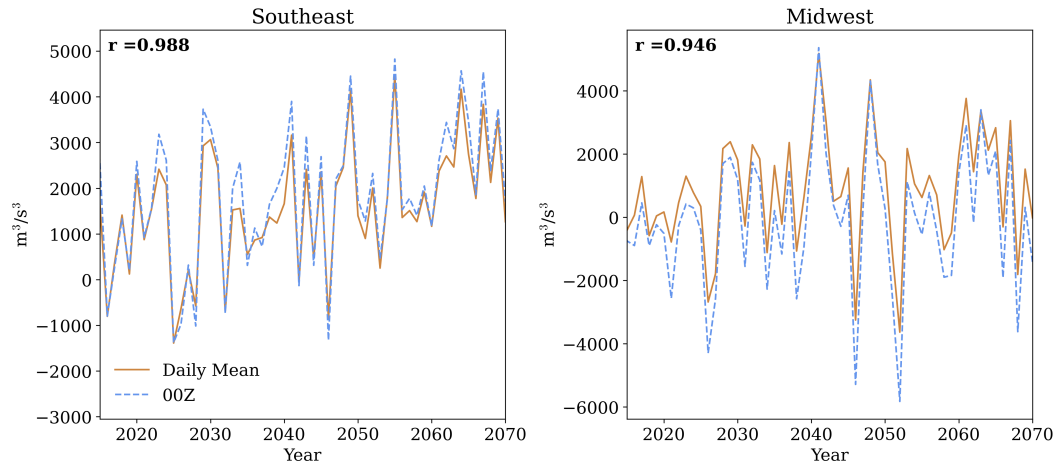


Figure 2: Time series of CAPES06 anomalies in the Southeast in MAM and in the Midwest in JJA from 2015-2070 from one member of the CESM2 Large Ensemble. Anomalies are relative to the 2015-2034 mean. The tan line represents CAPES06 anomalies calculated from daily mean data, while the blue dashed line represents CAPES06 anomalies from 00 Z data only. The correlation between the two time series is the r-value in the top left of each graph.

243 changes over time of the parameters computed from daily mean data, as well as the  
 244 differences between the SAI and no-SAI simulations, are very similar to the temporal  
 245 changes of the parameters computed from 00 Z data only. Using the daily mean data that  
 246 is available from all 10 ARISE-SAI ensemble members for a better estimation of the  
 247 forced changes in climate, as well as to better examine how the forced changes might be  
 248 modified by decadal and multi-decadal internal climate variability.

### 249 **3 Results**

#### 250 **3.1 Forced Responses**

251 Differences in future projections with and without SAI are evident in many convective  
 252 weather environment parameters averaged over the Southeast and Midwest regions  
 253 (Figure 3). Without SAI deployment, MUCAPE increases throughout the time period  
 254 relative to the base period (2015-2034), but with SAI deployment MUCAPE stabilizes  
 255 (Figure 3a, 3e). Similarly, climate change causes an increase in the magnitude of MUCIN  
 256 (increasingly negative values) in both regions while SAI stabilizes MUCIN near 2035 levels

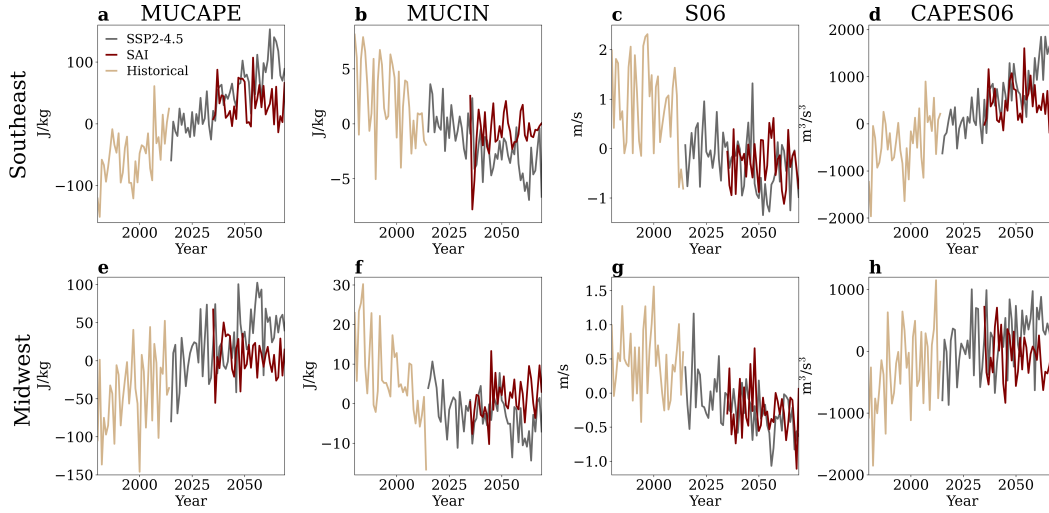


Figure 3: Time series showing MUCAPE ( $\text{J kg}^{-1}$ ) (a and e), MUCIN ( $\text{J kg}^{-1}$ ) (b and f), S06 ( $\text{m s}^{-1}$ ) (c and g), and CAPES06 ( $\text{m}^3 \text{s}^{-3}$ ) (d and h) anomalies relative to the 2015-2034 mean for the Southeast in MAM (top row) and the Midwest in JJA (bottom row) from 1980-2069. The tan line represents the three-member ensemble mean from CESM2(WACCM6) historical runs, the gray line represents the 10-member ensemble mean from the SSP2-4.5 simulations, and the red line represents the 10-member ensemble mean from the simulations with SAI deployment beginning in 2035.

257 in these simulations (Figure 3b, 3f). S06 decreases in magnitude throughout the time  
 258 period in the no-SAI simulations, but the influence of SAI on wind shear is less clear  
 259 (Figure 3c, 3g). The sign of future greenhouse-gas induced changes in MUCAPE, MUCIN  
 260 and S06 are in general agreement with previous studies (Diffenbaugh et al., 2013; Lepore  
 261 et al., 2021; Trapp et al., 2009; K. L. Rasmussen et al., 2017), although magnitudes differ,  
 262 partly because earlier studies examined climate change scenarios other than SSP2-4.5 and  
 263 with a variety of model frameworks. Projected increases in the magnitude of CAPES06,  
 264 which are dominated by increases in MUCAPE with continued climate warming (Figure  
 265 3d, 3h) are also in line with earlier studies (Diffenbaugh et al., 2013; Seeley & Romps,  
 266 2015; Trapp et al., 2007). It thus follows that changes in CAPES06 mirror the simulated  
 267 changes to MUCAPE in the SAI runs, with anomalies stabilizing to approximately 2035  
 268 levels (Figure 3d, 3h).

269 The underlying climatological (2015-2034) spatial distributions of these parameters from  
 270 the ARISE-SAI simulations (Figure 4) provide context for projected changes with and

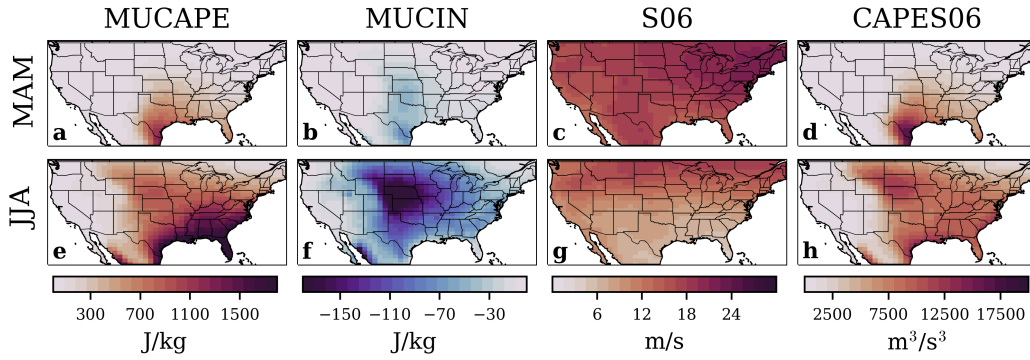


Figure 4: Climatological MUCAPE (a and e), MUCIN (b and f), S06 (c and g) and CAPES06 (d and h) for MAM (top row) and JJA (bottom row) over 2015-2034 for the SSP2-4.5 simulations.

271 without SAI, and they are in good agreement with observations (e.g., Franke et al., 2023;  
 272 Li et al., 2020; Chen et al., 2020; K. L. Rasmussen et al., 2017). In MAM, maximum  
 273 values of MUCAPE are found over the south-central U.S., especially just west of the Gulf  
 274 of Mexico (Figure 4a). The area of maximum MUCAPE becomes much larger in JJA,  
 275 with large values generally east of the Rockies and the greatest magnitudes over the far  
 276 southern U.S. (Figure 4e). The changes between MAM and JJA are especially notable  
 277 over the Northern Plains and the Midwest, where MUCAPE in the summer has  
 278 magnitudes near those of the Southeast in MAM (Figure 4e).

279 Similar to MUCAPE, the magnitude of MUCIN increases greatly from MAM to JJA  
 280 (Figure 4b, 4f), although again note the magnitudes of the climatological values from  
 281 daily mean data are larger than in previous studies that have utilized data from the  
 282 afternoon only. In particular, the largest magnitudes of MUCIN are concentrated over  
 283 Texas, Oklahoma and Kansas in MAM, but by JJA the largest magnitudes are shifted to  
 284 the central Great Plains. S06 is positive over the entire U.S. during both seasons,  
 285 although it is larger in spring than summer (Figure 4c, 4g). In both seasons, maximum  
 286 values of wind shear are over the northern third of the U.S. The distribution of CAPES06  
 287 largely mirrors the distribution of MUCAPE in both MAM and JJA (Figure 4d, 4h),  
 288 although CAPES06 has a more uniform distribution across the eastern half of the U.S. in  
 289 JJA compared to MUCAPE (4d, 4h).

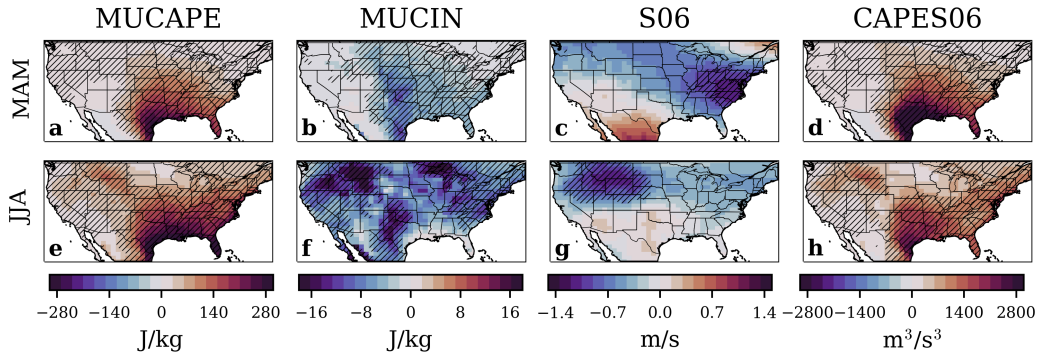


Figure 5: The differences between 2060-2069 (SSP2-4.5) and 2015-2034 (SSP2-4.5) ensemble mean MUCAPE, MUCIN, S06, and CAPES06, in MAM (top row) and JJA (bottom row). Stippling indicates statistical significance at the  $\alpha=0.05$  level.

290 To examine how climate change affects these environmental parameters, the average  
 291 changes in the last decade of the ARISE-SAI simulations (2060-2069) are examined  
 292 relative to the climatological period (2015-2034; Figure 5). In the spring and summer,  
 293 MUCAPE, MUCIN, and CAPES06 are all projected to increase in magnitude with  
 294 climate change (Figure 5). Over most regions, these increases are statistically significant  
 295 at the  $\alpha=0.05$  level for the two-sample t-test (to account for issues related to multiple  
 296 testing across the U.S. domain, the method outlined in Wilks (2016) was used to control  
 297 the false discovery rate). Wind shear (S06) is projected to decrease in magnitude during  
 298 MAM across much of the U.S., with decreases largest in the eastern U.S. (Figure 5c). S06  
 299 is also projected to decrease in the summer months, with the largest decreases in the  
 300 northwest U.S. where convective activity is not as significant historically (Figure 5g).  
 301 While decreases in wind shear are evident across much of the U.S., the magnitude of the  
 302 decrease is relatively small compared to the magnitude of the underlying climatology  
 303 (Figure 4c, 4g, 5c, 5g): climatological S06 values exceed  $20 \text{ m s}^{-1}$  across much of the U.S.,  
 304 while projected changes by 2060-2069 exceed  $1 \text{ m s}^{-1}$  over only limited regions (Figure 5c,  
 305 5g). Projected increases in MUCAPE, MUCIN and CAPES06, as well as projected  
 306 decreases in S06, are broadly consistent with previous literature (Difffenbaugh et al., 2013;  
 307 Franke et al., 2023; Hoogewind et al., 2017; Lepore et al., 2021; K. L. Rasmussen et al.,  
 308 2017; Seeley & Romps, 2015; Trapp et al., 2007, 2009).

309 In the SAI simulations, future changes in the magnitudes in MUCAPE, MUCIN and  
310 CAPES06 are generally much smaller and less statistically significant across the U.S.  
311 (Figure 6) than in the no-SAI simulations (Figure 5). This suggests that if SAI were to be  
312 deployed, the convective weather environment parameters analyzed here would not change  
313 appreciably from today, although that conclusion may be specific to the ARISE-SAI  
314 simulations. Future changes in S06 with SAI, however, are generally similar to those  
315 projected in the no-SAI simulations. For instance, the spatial patterns of projected  
316 decreases in S06 with SAI are similar to those without SAI in MAM (Figure 5c, 6c),  
317 although regions of maximum decrease differ. Since an objective of the ARISE-SAI  
318 experiment is to not only keep global average temperature near its 2035 value but also to  
319 preserve the equator-to-pole temperature gradient (Richter et al., 2022), it is difficult to  
320 simply attribute the S06 decreases in the no-SAI simulations (Figure 5c) to changes in the  
321 thermal wind balance, as has been done previously (Trapp et al., 2007; Seeley & Romps,  
322 2015). The results suggest that there could be a different mechanism driving future  
323 changes in S06 that has not previously been identified. This aspect is further explored in  
324 the Discussion section.

325 Another way to examine the impacts of SAI on convective weather environment  
326 parameters relative to the effects from increasing greenhouse concentrations alone is to  
327 directly difference the SAI and no-SAI simulations. Here this is done for differences  
328 averaged over the 2060-2069 decade. For MUCAPE, MUCIN, and CAPES06, the  
329 differences follow a similar spatial pattern and magnitude, but are of the opposite sign, to  
330 the projected future changes in the no-SAI simulations (Figure 5 and 7). Further, the  
331 differences between the SAI and no-SAI simulations for MUCAPE, MUCIN and  
332 CAPES06 are widely statistically significant across the eastern U.S. for 2060-2069, while  
333 the differences for S06 are not (Figure 7).

334 In addition to examining changes in each convective weather environment parameter  
335 separately, understanding their co-variability can provide insight into the potential change  
336 in the distributions of convective modes and frequency with and without SAI  
337 (Difffenbaugh et al., 2013; Lepore et al., 2021; K. L. Rasmussen et al., 2017). To this  
338 point, bivariate distributions of convective weather environment parameters from  
339 2060-2069 were created from daily data for the SAI and no-SAI simulations, respectively.  
340 For each individual ensemble member, daily mean values of MUCAPE, MUCIN and S06  
341 were collected for each gridpoint over the Southeast in MAM and the Midwest in JJA.

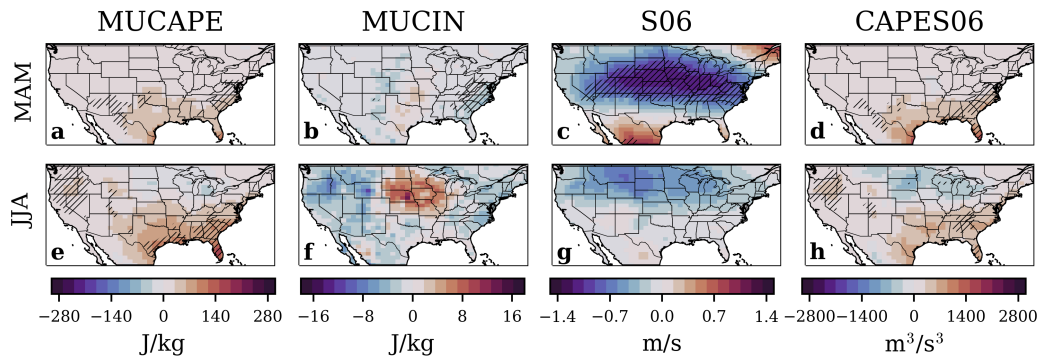


Figure 6: Differences between 2060-2069 (SAI) and 2015-2034 (SSP2-4.5) ensemble mean MUCAPE, MUCIN, S06, and CAPES06, in MAM (top row) and JJA (bottom row). Stippling indicates statistical significance at the  $\alpha=0.05$  level.

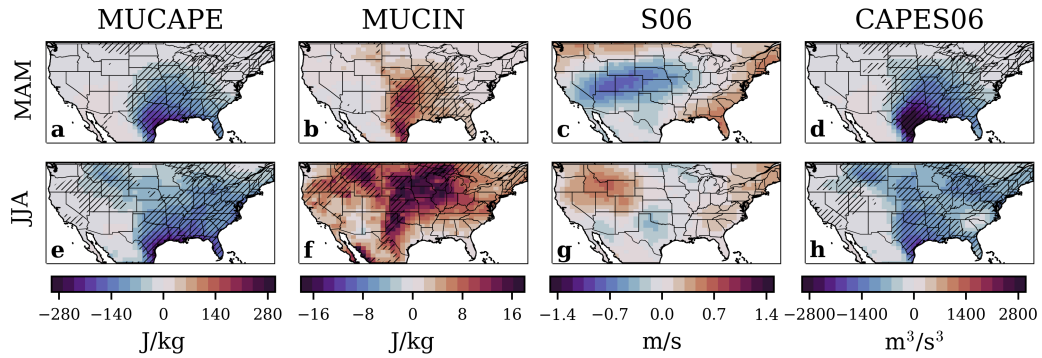


Figure 7: Differences between SAI and SSP2-4.5 ensemble means for 2060-2069 in MAM (top row) and JJA (bottom row). Stippling indicates statistical significance at the  $\alpha=0.05$  level.

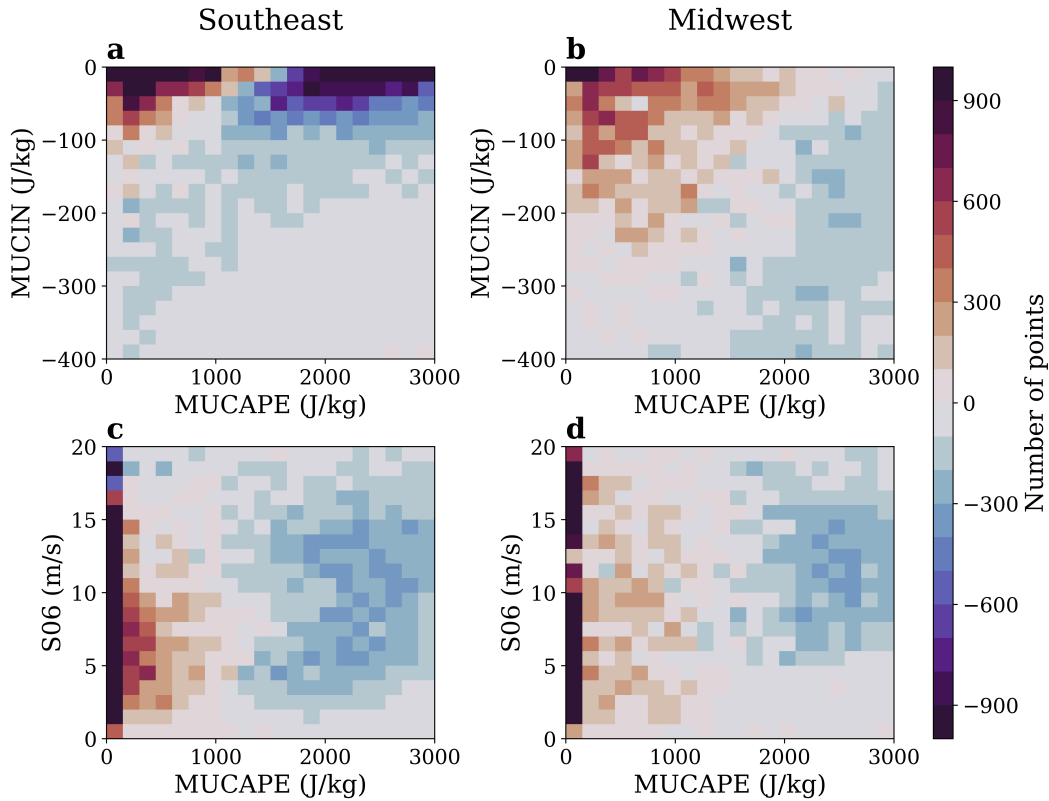


Figure 8: The difference between the SAI and no-SAI simulations (i.e., SAI - SSP2-4.5) for the bivariate distribution of MUCAPE (x-axis) and MUCIN (y-axis) for the Southeast in MAM (a) and the Midwest in JJA (b) over 2060-2069. (c) shows the difference between the SAI and no-SAI simulations for the bivariate distribution of MUCAPE (x-axis) and S06 (y-axis) for the Southeast in MAM, while (d) shows the same, but for the Midwest in JJA. Red (blue) pixels represent bins where there are more (less) days with corresponding MUCAPE and MUCIN (MUCAPE and S06) values in the simulations with SAI.

342 Distinct bivariate distributions (MUCAPE versus MUCIN, and MUCAPE versus S06)  
 343 were then plotted for the difference of the SAI and no-SAI simulations (Figure 8).  
 344 Positive numbers indicate that the SAI simulations had more days in a given bin than the  
 345 no-SAI simulations, whereas negative numbers indicate the opposite.

346 In the Southeast in MAM and the Midwest in JJA, there are more days with low  
 347 magnitudes of MUCAPE and MUCIN in the SAI simulations than in the no-SAI  
 348 simulations, indicating that projected increases in the number of days with increased  
 349 MUCAPE and MUCIN magnitudes under SSP2-4.5 could be largely avoided with SAI

(Figure 8a, 8b). The shift in the distribution of these parameters is due to decreases in both MUCAPE and MUCIN, which is evident in the straight diagonal region that separates the red and blue points. The difference in the shape of the distributions between the Southeast in MAM (Figure 8a) and the Midwest in JJA (Figure 8b) is largely due to the climatology of MUCIN, where values have much higher magnitudes in the Midwest in JJA (Figure 4b, 4f).

The difference between the SAI and no-SAI simulations for the daily bivariate distribution of MUCAPE and S06 is illustrated in Figure 8c and 8d. While the simulations suggest fewer days with high MUCAPE if SAI were to be deployed, the number of days with high shear is comparable between the SAI and no-SAI simulations. Thus, with SAI, there may be fewer days with high magnitude MUCAPE and S06, but the number of days with low-to-moderate MUCAPE and high shear may be similar with and without SAI (Figure 8c, 8d).

The analyses in Figure 8 also begin to highlight the potential role of unforced, internal climate variability in projected future changes in convective weather environments with and without SAI. The potential for internal variability to significantly modulate projected forced changes in climate is known to be significant (e.g. Deser et al., 2012; Deser, 2020; Schwarzwald and Lenssen, 2022). Motivated by these and similar studies, the next section goes beyond descriptions of only forced changes in climate warming in order to more completely examine the range of plausible future convective weather environments with and without SAI.

### 3.2 The Role of Internal Climate Variability

Other studies have examined the impact of internal climate variability on the behavior of severe weather related phenomena. However, they have tended to focus on sub-seasonal-to-interannual variations, such as those associated with the Madden Julian Oscillation (Baggett et al., 2018; Thompson & Roundy, 2013) or the El Niño Southern Oscillation (ENSO) phenomenon. For instance, J. T. Allen et al. (2018) examined the role of ENSO in modulating the annual cycle of tornadoes over the U.S., while Tippett et al. (2022) studied how ENSO and the phase of the Arctic Oscillation (AO) impacted the predictability of the tornado environment index. What has not been often considered, however, is the potential role that lower frequency (e.g., decadal) internal climate

381 variability could play in future projections of severe weather. Ensemble simulations from  
382 climate and Earth system models indicate that even though the forced response to  
383 increasing greenhouse gas concentrations shows warming across the U.S. and other land  
384 regions, decadal and longer-timescale internal climate variability has the potential to  
385 significantly enhance or dampen the forced response (Deser et al., 2012; Hawkins &  
386 Sutton, 2009; Kay et al., 2015). It is thus relevant to consider how internal climate  
387 variability may impact future projections of convective weather environments both with  
388 and without SAI.

389 Histograms of changes in MUCAPE and CAPES06 by 2060-2069 relative to the reference  
390 period (2015-2034) show that while the forced response (ensemble mean) increases in  
391 magnitude under SSP2-4.5, changes in individual no-SAI simulations could be notably  
392 smaller or larger due to unforced variations in climate (Figure 9; gray bars). Specifically,  
393 individual ensemble members project changes in MUCAPE that depart as much as  $60 \text{ J}$   
394  $\text{kg}^{-1}$  from the ensemble mean increase of  $107 \text{ J kg}^{-1}$  by 2060-2069 over the Southeast in  
395 MAM (Figure 9a). Similar results are evident for CAPES06. For instance, while the  
396 ensemble-mean projected change in CAPES06 is an increase of  $392 \text{ m}^3 \text{ s}^{-3}$  across the  
397 Midwest in JJA, one member projects a decrease of  $226 \text{ m}^3 \text{ s}^{-3}$  by mid-century (Figure  
398 9h). Such results confirm the large role that internal climate variability will likely play in  
399 the future evolution of climate, a point also emphasized recently by Franke et al. (2023)  
400 who examined future decadal trends in convective environment variables using the  
401 CESM2 Large Ensemble under SSP3-7.0 (Rodgers et al., 2021).

402 A similarly wide range of possible changes in MUCAPE, MUCIN and CAPES06 are also  
403 evident in the SAI simulations (Figure 9; red hatched bars). Thus, while the forced  
404 signals in the convective weather environment parameters examined here are distinct in  
405 future worlds with and without SAI, internal climate variability could produce similar  
406 climate outcomes in the decades ahead (Keys et al., 2022). For example, an ensemble  
407 member in the no-SAI simulation projects that MUCIN decreases in magnitude by  $5.2 \text{ J}$   
408  $\text{kg}^{-1}$  in the Midwest in JJA by 2060-2069, while a member in the SAI simulation projects  
409 an  $8.5 \text{ J kg}^{-1}$  increase in MUCIN over the same period (Figure 9f). Additionally, the  
410 distribution of possible future changes in S06 with and without SAI are very similar  
411 across ARISE-SAI ensemble members when averaged over the Southeast and Midwest  
412 regions, as is the case for the ensemble-mean changes (Figure 9c, 9g). This further

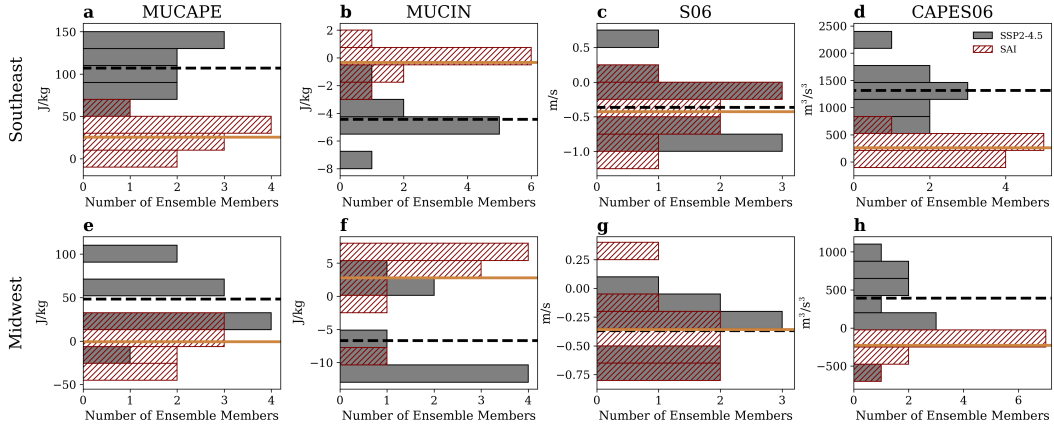


Figure 9: Histograms of the 10 ensemble members of the SSP2-4.5 (gray bars) and SAI (red hatched bars) simulations, illustrating the change in MUCAPE, MUCIN, S06, and CAPES06 for 2060-2069 relative to the 2015-2034. The black dotted and solid tan lines represent the ensemble mean values of the SSP2-4.5 and SAI simulations, respectively. Results are for the Southeast in MAM (a-d) and the Midwest in JJA (f-h).

413 supports the idea that the thermal wind relationship may not be the primary mechanism  
 414 governing future changes in the deep-layer tropospheric wind shear over the U.S.

415 To further illustrate the extent to which internal climate variability can produce a climate  
 416 outcome that differs significantly from the forced response alone, the ensemble member  
 417 with the maximum change in CAPES06 by 2060-2069 when averaged over the Southeast  
 418 in MAM is contrasted against the ensemble member with the smallest change. The spatial  
 419 patterns of change for each of these two ensemble members is shown in Figure 10, along  
 420 with the ensemble mean changes. By subtracting the latter from the total changes in  
 421 CAPES06, the regional changes due only to internal climate variability are revealed. The  
 422 main point is that internal climate variability may either significantly enhance the forced  
 423 response due to climate change (Figure 10c) or suppress it (Figure 10f) on decadal time  
 424 scales. It is also notable that the magnitudes of the changes due solely to internal climate  
 425 variability are spatially coherent over large regions, and they are of similar magnitude to  
 426 the force changes (e.g., Deser et al., 2020).

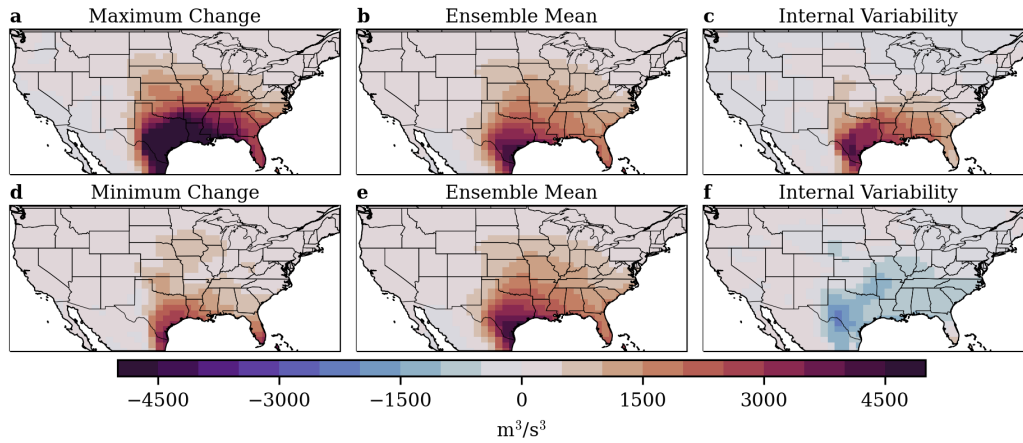


Figure 10: The ensemble members with the maximum (a) and minimum (b) changes in CAPES06 by 2060-2069 relative to 2015-2034 over the Southeast in MAM in the SSP2-4.5 simulations, calculation described in text. The forced response, or ensemble mean, is shown in (b) and repeated in (e). The change in CAPES06 due only to internal variability is shown for the ensemble member with the maximum and minimum change in (c) and (f), respectively.

#### 4 Discussion

In ARISE-SAI, projected future changes in MUCAPE, MUCIN, and CAPES06 are smaller with simulated SAI deployment than what is projected with climate change alone (Figure 5, 6). This is consistent with lower temperatures and dew points on average throughout the troposphere in MAM and JJA in an SAI future (Figure S2). It thus follows that the SAI simulations have fewer co-occurrences of high magnitude MUCAPE and MUCIN in the future (Figure 8a, 8b), whereas changes in the bivariate distribution of MUCAPE and S06 are primarily driven by smaller values of MUCAPE in a future with SAI (Figure 8c, 8d).

Future differences in tropospheric wind shear are more difficult to understand than SAI-induced changes in thermodynamic parameters. Under climate change with and without SAI, S06 is expected to decrease across much of the convectively active regions in the U.S. in the spring and summer seasons (Figure 5c, 5g, 6c, 6g). Although the decreases are small in magnitude relative to the climatology (Figure 4c, 4g), similar decreases have been documented in other studies of future climate change. Trapp et al. (2007), for

442 instance, concluded that future decreases in tropospheric wind shear are consistent with  
443 decreases in the middle latitude thermal wind, as would be expected as the  
444 equator-to-pole temperature gradient decreases over the 21st century (Cohen et al., 2014;  
445 Francis & Vavrus, 2012). However, changes in S06 with SAI are broadly consistent with  
446 those in the no-SAI simulations examined here (Figure 5c, 5g, 6c, 6g), even though  
447 ARISE-SAI is configured so that the equator-to-pole temperature gradient remains near  
448 its 2035 value when SAI is deployed (Richter et al., 2022).

449 While a detailed analysis of the changes in wind shear are beyond the scope of this study,  
450 note that precipitation is projected to increase over the eastern equatorial Pacific during  
451 the seasons examined here under both the SAI and no-SAI simulations, although the  
452 increases projected with SAI are smaller in magnitude (Figure S3; see also Richter et al.,  
453 2022). Simpson et al. (2019) also indicated that precipitation is projected to increase in  
454 magnitude in the eastern equatorial Pacific in a future with SAI. Further, they examined  
455 the precipitation response to the addition of stratospheric heating in the absence of a  
456 greenhouse gas forcing, and found that precipitation is also projected to increase in the  
457 eastern equatorial Pacific. This suggests that precipitation changes in this region are  
458 influenced by dynamical responses that may result from the introduction of aerosols into  
459 the stratosphere. Upper-level divergence due to tropical convective heating in the  
460 equatorial Pacific can be the source of anomalous vorticity that drives the propagation of  
461 Rossby wave trains that impact the extratropics (Qin & Robinson, 1993; Sardeshmukh &  
462 Hoskins, 1988). This idea is broadly consistent with the spatial patterns of 300 hPa winds  
463 in both the SAI and no-SAI simulations, with alternating bands of increasing and  
464 decreasing winds emanating from the eastern tropical Pacific (Figure S4). In other words,  
465 future changes in S06 in the SAI and no-SAI simulations may be driven by changes in  
466 tropical precipitation and associated large-scale climate circulations, which are similar  
467 whether or not SAI is deployed.

468 A novel aspect of this study is the use of individual ensemble members to examine the  
469 variability around the forced responses to climate change and SAI in large-scale convective  
470 weather environment parameters relevant to severe weather (Figure 9). Recall that each  
471 individual ensemble member represents an equally-plausible climate outcome in the  
472 decades ahead (e.g., Deser et al., 2020). The results illustrate the large-role internal  
473 climate variability will likely have, especially on regional scales. This also means that  
474 future convective weather environments in an SAI world could be indistinguishable from a

475 world without SAI, even though the forced responses are distinguishable. Note that a  
476 10-member ensemble is likely insufficient to statistically capture the full breadth of  
477 possible outcomes (Deser et al., 2012; Franke et al., 2023). There are also shortcomings in  
478 the ability of Earth-system models to accurately represent internal climate variability  
479 (Orbe et al., 2020; O'Reilly et al., 2021).

480 Other limitations of this study include the fact that the use of large-scale parameters to  
481 assess how the behavior of severe weather may change in the future is itself a caveat, since  
482 a favorable environment does not imply that convection will actually occur. Further, this  
483 method assumes that the frequency of convective initiation will not change with climate  
484 warming (Hoogewind et al., 2017; Trapp et al., 2007, 2009), and that the rate of initiation  
485 would not be affected by SAI deployment. Convective initiation is dependent on a variety  
486 of factors such as orography and large-scale dynamics, the latter of which have the  
487 potential to be impacted by climate warming and potential SAI deployment. The  
488 representation of convective initiation is also likely sensitive to model configuration  
489 (Carlson et al., 1983; Trapp et al., 2007).

## 490 **5 Conclusion**

491 The potential impact of SAI on future convective weather environments across the U.S.  
492 Midwest and Southeast was evaluated in one climate change scenario, with and without  
493 SAI deployment. The ARISE-SAI simulations indicate that, with climate change,  
494 thermodynamic parameters such as MUCAPE and MUCIN are projected to increase in  
495 magnitude across the U.S. in the spring and summer, and that these increases could be  
496 mostly avoided if SAI were to be deployed. Future changes in kinematic parameters, such  
497 as S06, appear to be primarily driven by changes in precipitation over the eastern tropical  
498 Pacific, which are similar between climate change simulations with and without SAI.  
499 Results further indicate that internal climate variability has the potential to significantly  
500 impact future projections of U.S. convective weather environments regionally, with  
501 spatially-coherent changes of similar magnitude to the forced responses.

502 Future work could examine how model-specific biases impact future projections of  
503 convective weather environments with and without SAI. For instance, the exact  
504 ARISE-SAI scenarios examined here were recently completed using the first version of the  
505 U.K. Earth System Model (Archibald et al., 2020; Sellar et al., 2019; Henry et al., 2023).

506 It would also be insightful to examine Earth-system model simulations with different SAI  
507 deployment goals and timelines (e.g., MacMartin et al., 2022), as well as simulations  
508 under different climate change scenarios, such as the Stratospheric Aerosol Geoengineering  
509 Large Ensemble Project (Tilmes et al., 2018). Use of the output from Earth-system  
510 models to force high-resolution, regional climate models to explicitly examine how  
511 projected changes in the large-scale environment impact the distribution of convective  
512 modes could provide additional understanding as to how SAI deployment impacts  
513 convective weather (Ashley et al., 2023; Gensini et al., 2023; Gensini & Mote, 2015;  
514 K. L. Rasmussen et al., 2017; Trapp et al., 2019).

## 515 **6 Open Research**

516 The original ARISE-SAI data set from which the data in this work was derived (all SAI  
517 members and 5 no-SAI members) are located on the NCAR Climate Data Gateway  
518 (Richter, 2022a, <https://doi.org/10.5065/9kcn-9y79>). The remaining 5 no-SAI members  
519 are available from the NCAR Climate Data Gateway at (Richter, 2022b,  
520 <https://doi.org/10.26024/0cs0-ev98>). All ARISE-SAI data may also be accessed from  
521 Amazon Web Services (NCAR, 2022, [registry.opendata.aws/ncar-cesm2-arise/](https://registry.opendata.aws/ncar-cesm2-arise/)). The  
522 complete CESM2 (WACCM6) Historical runs from which the data in this work was  
523 derived are available at Earth System Grid (Danabasoglu, 2019,  
524 <https://doi.org/10.22033/ESGF/CMIP6.11298>).

## 525 **Acknowledgments**

526 This work was supported by the National Oceanic and Atmospheric Administration  
527 (NOAA grant #NA22OAR4320473) and the LAD Climate Group. The ARISE-SAI  
528 simulations were produced by the National Center for Atmospheric Research (NCAR)  
529 with support from the National Science Foundation (NSF; grant no. 1852977) and by  
530 SilverLining through its Safe Climate Research Initiative. The CESM2 (WACCM6)  
531 Historical simulations were produced by NCAR. The CESM project is supported  
532 primarily by NSF.

## 533 **References**

534 Abiodun, B. J., Odoulami, R. C., Sawadogo, W., Oloniyo, O. A., Abatan, A. A., New, M.,  
535 ... MacMartin, D. G. (2021, December). Potential impacts of stratospheric aerosol

536 injection on drought risk managements over major river basins in Africa. *Climatic*  
537 *Change*, 169(3), 31. Retrieved 2023-02-13, from  
538 <https://doi.org/10.1007/s10584-021-03268-w> doi:  
539 10.1007/s10584-021-03268-w

540 Allen, J. T., Molina, M. J., & Gensini, V. A. (2018). Modulation of Annual Cycle of  
541 Tornadoes by El Niño–Southern Oscillation. *Geophysical Research Letters*, 45(11),  
542 5708–5717. Retrieved 2023-03-30, from  
543 <https://onlinelibrary.wiley.com/doi/abs/10.1029/2018GL077482> (\_eprint:  
544 <https://onlinelibrary.wiley.com/doi/pdf/10.1029/2018GL077482>) doi:  
545 10.1029/2018GL077482

546 Allen, M. R., & Ingram, W. J. (2002, September). Constraints on future changes in  
547 climate and the hydrologic cycle. *Nature*, 419(6903), 224–232. Retrieved 2023-01-20,  
548 from <https://www.nature.com/articles/nature01092> (Number: 6903 Publisher:  
549 Nature Publishing Group) doi: 10.1038/nature01092

550 Archibald, A. T., O'Connor, F. M., Abraham, N. L., Archer-Nicholls, S., Chipperfield,  
551 M. P., Dalvi, M., ... Zeng, G. (2020, March). Description and evaluation of the  
552 UKCA stratosphere–troposphere chemistry scheme (StratTrop vn 1.0) implemented  
553 in UKESM1. *Geoscientific Model Development*, 13(3), 1223–1266. Retrieved  
554 2023-03-24, from <https://gmd.copernicus.org/articles/13/1223/2020/>  
555 (Publisher: Copernicus GmbH) doi: 10.5194/gmd-13-1223-2020

556 Ashley, W. S., Haberlie, A. M., & Gensini, V. A. (2023, January). The Future of  
557 Supercells in the United States. *Bulletin of the American Meteorological Society*,  
558 104(1), E1–E21. Retrieved 2023-01-17, from [https://journals.ametsoc.org/  
559 view/journals/bams/104/1/BAMS-D-22-0027.1.xml](https://journals.ametsoc.org/view/journals/bams/104/1/BAMS-D-22-0027.1.xml) doi:  
560 10.1175/BAMS-D-22-0027.1

561 Baggett, C. F., Nardi, K. M., Childs, S. J., Zito, S. N., Barnes, E. A., & Maloney, E. D.  
562 (2018). Skillful Subseasonal Forecasts of Weekly Tornado and Hail Activity Using  
563 the Madden-Julian Oscillation. *Journal of Geophysical Research: Atmospheres*,  
564 123(22), 12,661–12,675. Retrieved 2023-05-22, from  
565 <https://onlinelibrary.wiley.com/doi/abs/10.1029/2018JD029059> (\_eprint:  
566 <https://onlinelibrary.wiley.com/doi/pdf/10.1029/2018JD029059>) doi:  
567 10.1029/2018JD029059

568 Barnes, E. A., Hurrell, J. W., & Sun, L. (2022). Detecting Changes in Global Extremes

- 569 Under the GLENS-SAI Climate Intervention Strategy. *Geophysical Research*  
570 *Letters*, 49(20), e2022GL100198. Retrieved 2022-11-08, from  
571 <https://onlinelibrary.wiley.com/doi/abs/10.1029/2022GL100198> (\_eprint:  
572 <https://onlinelibrary.wiley.com/doi/pdf/10.1029/2022GL100198>) doi:  
573 10.1029/2022GL100198
- 574 Bednarz, E. M., Visioni, D., Richter, J. H., Butler, A. H., & MacMartin, D. G. (2022).  
575 Impact of the Latitude of Stratospheric Aerosol Injection on the Southern Annular  
576 Mode. *Geophysical Research Letters*, 49(19), e2022GL100353. Retrieved 2023-05-23,  
577 from <https://onlinelibrary.wiley.com/doi/abs/10.1029/2022GL100353>  
578 (\_eprint: <https://onlinelibrary.wiley.com/doi/pdf/10.1029/2022GL100353>) doi:  
579 10.1029/2022GL100353
- 580 Brooks, H. E., Anderson, A. R., Riemann, K., Ebberts, I., & Flachs, H. (2007, February).  
581 Climatological aspects of convective parameters from the NCAR/NCEP reanalysis.  
582 *Atmospheric Research*, 83(2), 294–305. Retrieved 2022-08-04, from  
583 <https://www.sciencedirect.com/science/article/pii/S0169809506001128>  
584 doi: 10.1016/j.atmosres.2005.08.005
- 585 Brooks, H. E., Doswell, C. A., & Kay, M. P. (2003, August). Climatological Estimates of  
586 Local Daily Tornado Probability for the United States. *Weather and Forecasting*,  
587 18(4), 626–640. Retrieved 2023-01-17, from [https://journals.ametsoc.org/  
588 view/journals/wefo/18/4/1520-0434\\_2003\\_018\\_0626\\_ceoldt\\_2\\_0\\_co\\_2.xml](https://journals.ametsoc.org/view/journals/wefo/18/4/1520-0434_2003_018_0626_ceoldt_2_0_co_2.xml)  
589 (Publisher: American Meteorological Society Section: Weather and Forecasting) doi:  
590 10.1175/1520-0434(2003)018<0626:CEOLDT>2.0.CO;2
- 591 Carlson, T. N., Benjamin, S. G., Forbes, G. S., & Li, Y.-F. (1983, July). Elevated Mixed  
592 Layers in the Regional Severe Storm Environment: Conceptual Model and Case  
593 Studies. *Monthly Weather Review*, 111(7), 1453–1474. Retrieved 2023-04-04, from  
594 [https://journals.ametsoc.org/view/journals/mwre/111/7/  
595 1520-0493\\_1983\\_111\\_1453\\_emlitr\\_2\\_0\\_co\\_2.xml](https://journals.ametsoc.org/view/journals/mwre/111/7/1520-0493_1983_111_1453_emlitr_2_0_co_2.xml) (Publisher: American  
596 Meteorological Society Section: Monthly Weather Review) doi:  
597 10.1175/1520-0493(1983)111<1453:EMLITR>2.0.CO;2
- 598 Chen, J., Dai, A., Zhang, Y., & Rasmussen, K. L. (2020, February). Changes in  
599 Convective Available Potential Energy and Convective Inhibition under Global  
600 Warming. *Journal of Climate*, 33(6), 2025–2050. Retrieved 2023-05-18, from  
601 <https://journals.ametsoc.org/view/journals/clim/33/6/>

- 602 jcli-d-19-0461.1.xml (Publisher: American Meteorological Society Section:  
603 Journal of Climate) doi: 10.1175/JCLI-D-19-0461.1
- 604 Cohen, J., Screen, J. A., Furtado, J. C., Barlow, M., Whittleston, D., Coumou, D., ...  
605 Jones, J. (2014, September). Recent Arctic amplification and extreme mid-latitude  
606 weather. *Nature Geoscience*, 7(9), 627–637. Retrieved 2023-05-01, from  
607 <https://www.nature.com/articles/ngeo2234> (Number: 9 Publisher: Nature  
608 Publishing Group) doi: 10.1038/ngeo2234
- 609 Craven, J. P., & Brooks, H. E. (2004). BASELINE CLIMATOLOGY OF SOUNDING  
610 DERIVED PARAMETERS ASSOCIATED WITH DEEP MOIST CONVECTION.  
611 *National Weather Digest*, 28.
- 612 Crutzen, P. J. (2006, August). Albedo Enhancement by Stratospheric Sulfur Injections:  
613 A Contribution to Resolve a Policy Dilemma? *Climatic Change*, 77(3-4), 211.  
614 Retrieved 2022-06-08, from  
615 <https://link.springer.com/10.1007/s10584-006-9101-y> doi:  
616 10.1007/s10584-006-9101-y
- 617 Danabasoglu, G. (2019). *NCAR CESM2-WACCM-FV2 model output prepared for CMIP6*  
618 *CMIP historical*. Earth System Grid Federation. Retrieved 2023-07-14, from  
619 <https://doi.org/10.22033/ESGF/CMIP6.11298> doi:  
620 10.22033/ESGF/CMIP6.11298
- 621 Danabasoglu, G., Lamarque, J.-F., Bacmeister, J., Bailey, D. A., DuVivier, A. K.,  
622 Edwards, J., ... Strand, W. G. (2020). The Community Earth System Model  
623 Version 2 (CESM2). *Journal of Advances in Modeling Earth Systems*, 12(2),  
624 e2019MS001916. Retrieved 2022-12-01, from  
625 <https://onlinelibrary.wiley.com/doi/abs/10.1029/2019MS001916> (eprint:  
626 <https://onlinelibrary.wiley.com/doi/pdf/10.1029/2019MS001916>) doi:  
627 10.1029/2019MS001916
- 628 Deser, C., Knutti, R., Solomon, S., & Phillips, A. S. (2012, November). Communication  
629 of the role of natural variability in future North American climate. *Nature Climate*  
630 *Change*, 2(11), 775–779. Retrieved 2023-03-21, from  
631 <https://www.nature.com/articles/nclimate1562> (Number: 11 Publisher:  
632 Nature Publishing Group) doi: 10.1038/nclimate1562
- 633 Deser, C., Lehner, F., Rodgers, K. B., Ault, T., Delworth, T. L., DiNezio, P. N., ... Ting,  
634 M. (2020, April). Insights from Earth system model initial-condition large

- 635 ensembles and future prospects. *Nature Climate Change*, *10*(4), 277–286. Retrieved  
636 2023-01-23, from <https://www.nature.com/articles/s41558-020-0731-2>  
637 (Number: 4 Publisher: Nature Publishing Group) doi: 10.1038/s41558-020-0731-2
- 638 Diffenbaugh, N. S., Scherer, M., & Trapp, R. J. (2013, October). Robust increases in  
639 severe thunderstorm environments in response to greenhouse forcing. *Proceedings of*  
640 *the National Academy of Sciences*, *110*(41), 16361–16366. Retrieved 2023-01-17,  
641 from <https://www.pnas.org/doi/10.1073/pnas.1307758110> (Publisher:  
642 Proceedings of the National Academy of Sciences) doi: 10.1073/pnas.1307758110
- 643 Donat, M. G., Lowry, A. L., Alexander, L. V., O’Gorman, P. A., & Maher, N. (2016,  
644 May). More extreme precipitation in the world’s dry and wet regions. *Nature*  
645 *Climate Change*, *6*(5), 508–513. Retrieved 2023-01-20, from  
646 <https://www.nature.com/articles/nclimate2941> (Number: 5 Publisher: Nature  
647 Publishing Group) doi: 10.1038/nclimate2941
- 648 Doswell, C. A., Brooks, H. E., & Kay, M. P. (2005, August). Climatological Estimates of  
649 Daily Local Nontornadic Severe Thunderstorm Probability for the United States.  
650 *Weather and Forecasting*, *20*(4), 577–595. Retrieved 2022-08-08, from  
651 <https://journals.ametsoc.org/view/journals/wefo/20/4/waf866.1.xml>  
652 (Publisher: American Meteorological Society Section: Weather and Forecasting) doi:  
653 10.1175/WAF866.1
- 654 Doswell, C. A., Brooks, H. E., & Maddox, R. A. (1996, December). Flash Flood  
655 Forecasting: An Ingredients-Based Methodology. *Weather and Forecasting*, *11*(4),  
656 560–581. Retrieved 2022-08-08, from [https://journals.ametsoc.org/view/  
657 journals/wefo/11/4/1520-0434\\_1996\\_011\\_0560\\_fffaib\\_2\\_0\\_co\\_2.xml](https://journals.ametsoc.org/view/journals/wefo/11/4/1520-0434_1996_011_0560_fffaib_2_0_co_2.xml) (Publisher:  
658 American Meteorological Society Section: Weather and Forecasting) doi:  
659 10.1175/1520-0434(1996)011<0560:FFFAIB>2.0.CO;2
- 660 Doswell, C. A., & Rasmussen, E. N. (1994, December). The Effect of Neglecting the  
661 Virtual Temperature Correction on CAPE Calculations. *Weather and Forecasting*,  
662 *9*(4), 625–629. Retrieved 2023-01-18, from [https://journals.ametsoc.org/view/  
663 journals/wefo/9/4/1520-0434\\_1994\\_009\\_0625\\_teontv\\_2\\_0\\_co\\_2.xml](https://journals.ametsoc.org/view/journals/wefo/9/4/1520-0434_1994_009_0625_teontv_2_0_co_2.xml) (Publisher:  
664 American Meteorological Society Section: Weather and Forecasting) doi:  
665 10.1175/1520-0434(1994)009<0625:TEONTV>2.0.CO;2
- 666 Dougherty, E., & Rasmussen, K. L. (2020, October). Changes in Future Flash  
667 Flood–Producing Storms in the United States. *Journal of Hydrometeorology*,

668 21(10), 2221–2236. Retrieved 2023-08-02, from  
 669 <https://journals.ametsoc.org/view/journals/hydr/21/10/jhmD200014.xml>  
 670 (Publisher: American Meteorological Society Section: Journal of Hydrometeorology)  
 671 doi: 10.1175/JHM-D-20-0014.1

672 Eyring, V., Bony, S., Meehl, G. A., Senior, C. A., Stevens, B., Stouffer, R. J., & Taylor,  
 673 K. E. (2016, May). Overview of the Coupled Model Intercomparison Project Phase  
 674 6 (CMIP6) experimental design and organization. *Geoscientific Model Development*,  
 675 9(5), 1937–1958. Retrieved 2023-04-03, from  
 676 <https://gmd.copernicus.org/articles/9/1937/2016/> (Publisher: Copernicus  
 677 GmbH) doi: 10.5194/gmd-9-1937-2016

678 Francis, J. A., & Vavrus, S. J. (2012). Evidence linking Arctic amplification to extreme  
 679 weather in mid-latitudes. *Geophysical Research Letters*, 39(6). Retrieved  
 680 2023-05-01, from  
 681 <https://onlinelibrary.wiley.com/doi/abs/10.1029/2012GL051000> (eprint:  
 682 <https://onlinelibrary.wiley.com/doi/pdf/10.1029/2012GL051000>) doi:  
 683 10.1029/2012GL051000

684 Franke, M. E., Hurrell, J. W., Rasmussen, K., & Sun, L. (2023, January). *Impacts of*  
 685 *Forced and Internal Climate Variability on Changes in Convective Environments*  
 686 *Over the Eastern United States* (preprint). Preprints. Retrieved 2023-05-04, from  
 687 [https://essopenarchive.org/users/578629/articles/](https://essopenarchive.org/users/578629/articles/620460-impacts-of-forced-and-internal-climate-variability-on-changes-in-convective-environments-over-the-eastern-united-states?commit=f280406d36d6436beeabb633ec5ae9f65dca7b99)  
 688 [620460-impacts-of-forced-and-internal-climate-variability-on-changes](https://essopenarchive.org/users/578629/articles/620460-impacts-of-forced-and-internal-climate-variability-on-changes-in-convective-environments-over-the-eastern-united-states?commit=f280406d36d6436beeabb633ec5ae9f65dca7b99)  
 689 [-in-convective-environments-over-the-eastern-united-states?commit=](https://essopenarchive.org/users/578629/articles/620460-impacts-of-forced-and-internal-climate-variability-on-changes-in-convective-environments-over-the-eastern-united-states?commit=f280406d36d6436beeabb633ec5ae9f65dca7b99)  
 690 [f280406d36d6436beeabb633ec5ae9f65dca7b99](https://essopenarchive.org/users/578629/articles/620460-impacts-of-forced-and-internal-climate-variability-on-changes-in-convective-environments-over-the-eastern-united-states?commit=f280406d36d6436beeabb633ec5ae9f65dca7b99) doi:  
 691 10.22541/essoar.167458066.68764316/v1

692 Friedlingstein, P., O’Sullivan, M., Jones, M. W., Andrew, R. M., Gregor, L., Hauck, J., ...  
 693 Zheng, B. (2022, November). Global Carbon Budget 2022. *Earth System Science*  
 694 *Data*, 14(11), 4811–4900. Retrieved 2023-02-08, from  
 695 <https://essd.copernicus.org/articles/14/4811/2022/> (Publisher: Copernicus  
 696 GmbH) doi: 10.5194/essd-14-4811-2022

697 Galway, J. G. (1989, December). The Evolution of Severe Thunderstorm Criteria within  
 698 the Weather Service. *Weather and Forecasting*, 4(4), 585–592. Retrieved 2023-05-23,  
 699 from [https://journals.ametsoc.org/view/journals/wefo/4/4/](https://journals.ametsoc.org/view/journals/wefo/4/4/1520-0434-1989_004_0585_teostc_2_0_co_2.xml)  
 700 [1520-0434-1989\\_004\\_0585\\_teostc\\_2\\_0\\_co\\_2.xml](https://journals.ametsoc.org/view/journals/wefo/4/4/1520-0434-1989_004_0585_teostc_2_0_co_2.xml) (Publisher: American

- 701 Meteorological Society Section: Weather and Forecasting) doi:  
 702 10.1175/1520-0434(1989)004<0585:TEOSTC>2.0.CO;2
- 703 Gensini, V. A., Haberlie, A. M., & Ashley, W. S. (2023, January). Convection-permitting  
 704 simulations of historical and possible future climate over the contiguous United  
 705 States. *Climate Dynamics*, *60*(1), 109–126. Retrieved 2023-01-17, from  
 706 <https://doi.org/10.1007/s00382-022-06306-0> doi: 10.1007/s00382-022-06306-0  
 707
- 708 Gensini, V. A., & Mote, T. L. (2015, March). Downscaled estimates of late 21st century  
 709 severe weather from CCSM3. *Climatic Change*, *129*(1), 307–321. Retrieved  
 710 2022-11-29, from <https://doi.org/10.1007/s10584-014-1320-z> doi:  
 711 10.1007/s10584-014-1320-z
- 712 Gettelman, A., Mills, M. J., Kinnison, D. E., Garcia, R. R., Smith, A. K., Marsh, D. R.,  
 713 ... Randel, W. J. (2019). The Whole Atmosphere Community Climate Model  
 714 Version 6 (WACCM6). *Journal of Geophysical Research: Atmospheres*, *124*(23),  
 715 12380–12403. Retrieved 2023-01-17, from  
 716 <https://onlinelibrary.wiley.com/doi/abs/10.1029/2019JD030943> (\_eprint:  
 717 <https://onlinelibrary.wiley.com/doi/pdf/10.1029/2019JD030943>) doi:  
 718 10.1029/2019JD030943
- 719 Hawkins, E., & Sutton, R. (2009, August). The Potential to Narrow Uncertainty in  
 720 Regional Climate Predictions. *Bulletin of the American Meteorological Society*,  
 721 *90*(8), 1095–1108. Retrieved 2023-04-03, from  
 722 [https://journals.ametsoc.org/view/journals/bams/90/8/2009bams2607\\_1.xml](https://journals.ametsoc.org/view/journals/bams/90/8/2009bams2607_1.xml)  
 723 (Publisher: American Meteorological Society Section: Bulletin of the American  
 724 Meteorological Society) doi: 10.1175/2009BAMS2607.1
- 725 Henry, M., Haywood, J., Jones, A., Dalvi, M., Wells, A., Vioni, D., ... Tye, M. (2023,  
 726 June). Comparison of UKESM1 and CESM2 Simulations Using the Same  
 727 Multi-Target Stratospheric Aerosol Injection Strategy. *EGUsphere*, 1–22. Retrieved  
 728 2023-08-07, from  
 729 <https://egusphere.copernicus.org/preprints/2023/egusphere-2023-980/>  
 730 (Publisher: Copernicus GmbH) doi: 10.5194/egusphere-2023-980
- 731 Hoogewind, K. A., Baldwin, M. E., & Trapp, R. J. (2017, December). The Impact of  
 732 Climate Change on Hazardous Convective Weather in the United States: Insight  
 733 from High-Resolution Dynamical Downscaling. *Journal of Climate*, *30*(24),

- 734 10081–10100. Retrieved 2023-01-24, from [https://journals.ametsoc.org/view/](https://journals.ametsoc.org/view/journals/clim/30/24/jcli-d-16-0885.1.xml)  
735 [journals/clim/30/24/jcli-d-16-0885.1.xml](https://journals.ametsoc.org/view/journals/clim/30/24/jcli-d-16-0885.1.xml) (Publisher: American  
736 Meteorological Society Section: Journal of Climate) doi: 10.1175/JCLI-D-16-0885.1  
737
- 738 Hueholt, D. M., Barnes, E. A., Hurrell, J. W., Richter, J. H., & Sun, L. (2023, February).  
739 *Assessing Outcomes in Stratospheric Aerosol Injection Scenarios Shortly After*  
740 *Deployment* (preprint). Preprints. Retrieved 2023-05-04, from  
741 [https://essopenarchive.org/users/580207/articles/621364-assessing](https://essopenarchive.org/users/580207/articles/621364-assessing-outcomes-in-stratospheric-aerosol-injection-scenarios-shortly-after-deployment?commit=cd38f22b1228a1414f057f4cb5c866be8991006f)  
742 [-outcomes-in-stratospheric-aerosol-injection-scenarios-shortly-after](https://essopenarchive.org/users/580207/articles/621364-assessing-outcomes-in-stratospheric-aerosol-injection-scenarios-shortly-after-deployment?commit=cd38f22b1228a1414f057f4cb5c866be8991006f)  
743 [-deployment?commit=cd38f22b1228a1414f057f4cb5c866be8991006f](https://essopenarchive.org/users/580207/articles/621364-assessing-outcomes-in-stratospheric-aerosol-injection-scenarios-shortly-after-deployment?commit=cd38f22b1228a1414f057f4cb5c866be8991006f) doi:  
744 10.22541/essoar.167591089.94758275/v1
- 745 IPCC. (2021). Summary for Policymakers.
- 746 Ji, D., Fang, S., Curry, C. L., Kashimura, H., Watanabe, S., Cole, J. N. S., . . . Moore,  
747 J. C. (2018, July). Extreme temperature and precipitation response to solar  
748 dimming and stratospheric aerosol geoengineering. *Atmospheric Chemistry and*  
749 *Physics*, 18(14), 10133–10156. Retrieved 2023-04-19, from  
750 <https://acp.copernicus.org/articles/18/10133/2018/> (Publisher: Copernicus  
751 GmbH) doi: 10.5194/acp-18-10133-2018
- 752 Jiang, X., & Guan, D. (2016). Determinants of global CO2 emissions growth. *Applied*  
753 *Energy*, 184(C), 1132–1141. Retrieved 2023-05-23, from  
754 [https://econpapers.repec.org/article/eeeappene/](https://econpapers.repec.org/article/eeeappene/v_3a184_3ay_3a2016_3ai_3ac_3ap_3a1132-1141.htm)  
755 [v\\_3a184\\_3ay\\_3a2016\\_3ai\\_3ac\\_3ap\\_3a1132-1141.htm](https://econpapers.repec.org/article/eeeappene/v_3a184_3ay_3a2016_3ai_3ac_3ap_3a1132-1141.htm) (Publisher: Elsevier)
- 756 Kay, J. E., Deser, C., Phillips, A., Mai, A., Hannay, C., Strand, G., . . . Vertenstein, M.  
757 (2015, August). The Community Earth System Model (CESM) Large Ensemble  
758 Project: A Community Resource for Studying Climate Change in the Presence of  
759 Internal Climate Variability. *Bulletin of the American Meteorological Society*, 96(8),  
760 1333–1349. Retrieved 2022-05-12, from [https://journals.ametsoc.org/view/](https://journals.ametsoc.org/view/journals/bams/96/8/bams-d-13-00255.1.xml)  
761 [journals/bams/96/8/bams-d-13-00255.1.xml](https://journals.ametsoc.org/view/journals/bams/96/8/bams-d-13-00255.1.xml) (Publisher: American  
762 Meteorological Society Section: Bulletin of the American Meteorological Society)  
763 doi: 10.1175/BAMS-D-13-00255.1
- 764 Kelly, D. L., Schaefer, J. T., & Doswell, C. A. (1985, November). Climatology of  
765 Nontornadic Severe Thunderstorm Events in the United States. *Monthly Weather*  
766 *Review*, 113(11), 1997–2014. Retrieved 2022-08-08, from

- 767 [https://journals.ametsoc.org/view/journals/mwre/113/11/](https://journals.ametsoc.org/view/journals/mwre/113/11/1520-0493-1985-113.1997_conste_2_0_co_2.xml)  
768 [1520-0493-1985-113.1997\\_conste\\_2\\_0\\_co\\_2.xml](https://journals.ametsoc.org/view/journals/mwre/113/11/1520-0493-1985-113.1997_conste_2_0_co_2.xml) (Publisher: American  
769 Meteorological Society Section: Monthly Weather Review) doi:  
770 [10.1175/1520-0493\(1985\)113<1997:CONSTE>2.0.CO;2](https://doi.org/10.1175/1520-0493(1985)113<1997:CONSTE>2.0.CO;2)
- 771 Keys, P. W., Barnes, E. A., Diffenbaugh, N. S., Hurrell, J. W., & Bell, C. M. (2022,  
772 October). Potential for perceived failure of stratospheric aerosol injection  
773 deployment. *Proceedings of the National Academy of Sciences*, *119*(40),  
774 e2210036119. Retrieved 2022-11-09, from  
775 <https://www.pnas.org/doi/full/10.1073/pnas.2210036119> (Publisher:  
776 Proceedings of the National Academy of Sciences) doi: [10.1073/pnas.2210036119](https://doi.org/10.1073/pnas.2210036119)
- 777 Kravitz, B., MacMartin, D. G., Mills, M. J., Richter, J. H., Tilmes, S., Lamarque, J.-F.,  
778 ... Vitt, F. (2017). First Simulations of Designing Stratospheric Sulfate Aerosol  
779 Geoengineering to Meet Multiple Simultaneous Climate Objectives. *Journal of*  
780 *Geophysical Research: Atmospheres*, *122*(23), 12,616–12,634. Retrieved 2023-04-20,  
781 from <https://onlinelibrary.wiley.com/doi/abs/10.1002/2017JD026874>  
782 (\_eprint: <https://onlinelibrary.wiley.com/doi/pdf/10.1002/2017JD026874>) doi:  
783 [10.1002/2017JD026874](https://doi.org/10.1002/2017JD026874)
- 784 Kravitz, B., Robock, A., Boucher, O., Schmidt, H., Taylor, K. E., Stenchikov, G., &  
785 Schulz, M. (2011). The Geoengineering Model Intercomparison Project (GeoMIP).  
786 *Atmospheric Science Letters*, *12*(2), 162–167. Retrieved 2023-04-20, from  
787 <https://onlinelibrary.wiley.com/doi/abs/10.1002/asl.316> (\_eprint:  
788 <https://onlinelibrary.wiley.com/doi/pdf/10.1002/asl.316>) doi: [10.1002/asl.316](https://doi.org/10.1002/asl.316)
- 789 Lee, W. R., MacMartin, D. G., Vioni, D., Kravitz, B., Chen, Y., Moore, J. C., ...  
790 Bailey, D. A. (2023). High-Latitude Stratospheric Aerosol Injection to Preserve the  
791 Arctic. *Earth's Future*, *11*(1), e2022EF003052. Retrieved 2023-04-19, from  
792 <https://onlinelibrary.wiley.com/doi/abs/10.1029/2022EF003052> (\_eprint:  
793 <https://onlinelibrary.wiley.com/doi/pdf/10.1029/2022EF003052>) doi:  
794 [10.1029/2022EF003052](https://doi.org/10.1029/2022EF003052)
- 795 Lepore, C., Abernathy, R., Henderson, N., Allen, J. T., & Tippett, M. K. (2021). Future  
796 Global Convective Environments in CMIP6 Models. *Earth's Future*, *9*(12),  
797 e2021EF002277. Retrieved 2022-06-27, from  
798 <https://onlinelibrary.wiley.com/doi/abs/10.1029/2021EF002277> (\_eprint:  
799 <https://onlinelibrary.wiley.com/doi/pdf/10.1029/2021EF002277>) doi:

800 10.1029/2021EF002277

801 Li, F., Chavas, D. R., Reed, K. A., & Li, D. T. D. (2020, October). Climatology of Severe  
802 Local Storm Environments and Synoptic-Scale Features over North America in  
803 ERA5 Reanalysis and CAM6 Simulation. *Journal of Climate*, *33*(19), 8339–8365.  
804 Retrieved 2023-04-25, from  
805 <https://journals.ametsoc.org/view/journals/clim/33/19/jcliD190986.xml>  
806 (Publisher: American Meteorological Society Section: Journal of Climate) doi:  
807 10.1175/JCLI-D-19-0986.1

808 Lockley, A., Xu, Y., Tilmes, S., Sugiyama, M., Rothman, D., & Hinds, A. (2022, July).  
809 18 Politically relevant solar geoengineering scenarios. *Socio-Environmental Systems*  
810 *Modelling*, *4*, 18127–18127. Retrieved 2022-08-10, from  
811 <https://sesmo.org/article/view/18127> doi: 10.18174/sesmo.18127

812 MacMartin, D. G., Kravitz, B., Keith, D. W., & Jarvis, A. (2014, July). Dynamics of the  
813 coupled human–climate system resulting from closed-loop control of solar  
814 geoengineering. *Climate Dynamics*, *43*(1), 243–258. Retrieved 2023-04-20, from  
815 <https://doi.org/10.1007/s00382-013-1822-9> doi: 10.1007/s00382-013-1822-9

816 MacMartin, D. G., Visoni, D., Kravitz, B., Richter, J., Felgenhauer, T., Lee, W. R., ...  
817 Sugiyama, M. (2022, August). Scenarios for modeling solar radiation modification.  
818 *Proceedings of the National Academy of Sciences*, *119*(33), e2202230119. Retrieved  
819 2022-08-10, from <https://www.pnas.org/doi/full/10.1073/pnas.2202230119>  
820 (Publisher: Proceedings of the National Academy of Sciences) doi:  
821 10.1073/pnas.2202230119

822 Marsh, P. T., Brooks, H. E., & Karoly, D. J. (2007). Assessment of the severe weather  
823 environment in North America simulated by a global climate model. *Atmospheric*  
824 *Science Letters*, *8*(4), 100–106. Retrieved 2023-05-23, from  
825 <https://onlinelibrary.wiley.com/doi/abs/10.1002/asl.159> (eprint:  
826 <https://rmets.onlinelibrary.wiley.com/doi/pdf/10.1002/asl.159>) doi: 10.1002/asl.159

827  
828 Moore, J. C., Yue, C., Zhao, L., Guo, X., Watanabe, S., & Ji, D. (2019). Greenland Ice  
829 Sheet Response to Stratospheric Aerosol Injection Geoengineering. *Earth's Future*,  
830 *7*(12), 1451–1463. Retrieved 2023-04-19, from  
831 <https://onlinelibrary.wiley.com/doi/abs/10.1029/2019EF001393> (eprint:  
832 <https://onlinelibrary.wiley.com/doi/pdf/10.1029/2019EF001393>) doi:

- 833 10.1029/2019EF001393
- 834 Mukherjee, S., Mishra, A., & Trenberth, K. E. (2018, June). Climate Change and  
835 Drought: a Perspective on Drought Indices. *Current Climate Change Reports*, 4(2),  
836 145–163. Retrieved 2023-01-20, from  
837 <https://doi.org/10.1007/s40641-018-0098-x> doi: 10.1007/s40641-018-0098-x
- 838 NASEM. (2021). *Reflecting Sunlight: Recommendations for Solar Geoengineering*  
839 *Research and Research Governance*. Washington, D.C.: National Academies Press.  
840 Retrieved 2023-01-25, from <https://www.nap.edu/catalog/25762> doi:  
841 10.17226/25762
- 842 NCAR. (2022). *Community Earth System Model v2 ARISE (CESM2 ARISE) - Registry*  
843 *of Open Data on AWS*. Retrieved 2023-07-14, from  
844 <https://registry.opendata.aws/ncar-cesm2-arise/>
- 845 NCEI, A. B. (2022). *U.S. Billion-dollar Weather and Climate Disasters, 1980 - present*  
846 *(NCEI Accession 0209268)*. NOAA National Centers for Environmental  
847 Information. Retrieved 2023-01-20, from  
848 <https://www.ncei.noaa.gov/archive/accession/0209268> doi:  
849 10.25921/STKW-7W73
- 850 Orbe, C., Roedel, L. V., Adames, F., Dezfuli, A., Fasullo, J., Gleckler, P. J., ... Zhao, M.  
851 (2020, September). Representation of Modes of Variability in Six U.S. Climate  
852 Models. *Journal of Climate*, 33(17), 7591–7617. Retrieved 2023-04-04, from  
853 <https://journals.ametsoc.org/view/journals/clim/33/17/jcliD190956.xml>  
854 (Publisher: American Meteorological Society Section: Journal of Climate) doi:  
855 10.1175/JCLI-D-19-0956.1
- 856 O'Neill, B. C., Kriegler, E., Ebi, K. L., Kemp-Benedict, E., Riahi, K., Rothman, D. S., ...  
857 Solecki, W. (2017, January). The roads ahead: Narratives for shared socioeconomic  
858 pathways describing world futures in the 21st century. *Global Environmental*  
859 *Change*, 42, 169–180. Retrieved 2023-04-03, from  
860 <https://www.sciencedirect.com/science/article/pii/S0959378015000060>  
861 doi: 10.1016/j.gloenvcha.2015.01.004
- 862 O'Reilly, C. H., Befort, D. J., Weisheimer, A., Woollings, T., Ballinger, A., & Hegerl, G.  
863 (2021, September). Projections of northern hemisphere extratropical climate  
864 underestimate internal variability and associated uncertainty. *Communications*  
865 *Earth & Environment*, 2(1), 1–9. Retrieved 2023-03-30, from

- 866 <https://www.nature.com/articles/s43247-021-00268-7> (Number: 1 Publisher:  
867 Nature Publishing Group) doi: 10.1038/s43247-021-00268-7
- 868 Peters, G. P., Marland, G., Le Quéré, C., Boden, T., Canadell, J. G., & Raupach, M. R.  
869 (2012, January). Rapid growth in CO<sub>2</sub> emissions after the 2008–2009 global  
870 financial crisis. *Nature Climate Change*, *2*(1), 2–4. Retrieved 2023-05-23, from  
871 <https://www.nature.com/articles/nclimate1332> (Number: 1 Publisher: Nature  
872 Publishing Group) doi: 10.1038/nclimate1332
- 873 Prein, A. F., Rasmussen, R. M., Ikeda, K., Liu, C., Clark, M. P., & Holland, G. J. (2017,  
874 January). The future intensification of hourly precipitation extremes. *Nature*  
875 *Climate Change*, *7*(1), 48–52. Retrieved 2023-08-02, from  
876 <https://www.nature.com/articles/nclimate3168> (Number: 1 Publisher: Nature  
877 Publishing Group) doi: 10.1038/nclimate3168
- 878 Qin, J., & Robinson, W. A. (1993, June). On the Rossby Wave Source and the Steady  
879 Linear Response to Tropical Forcing. *Journal of the Atmospheric Sciences*, *50*(12),  
880 1819–1823. Retrieved 2022-09-19, from [https://journals.ametsoc.org/view/  
881 journals/atsc/50/12/1520-0469\\_1993\\_050\\_1819\\_otrwsa\\_2\\_0\\_co\\_2.xml](https://journals.ametsoc.org/view/journals/atsc/50/12/1520-0469_1993_050_1819_otrwsa_2_0_co_2.xml)  
882 (Publisher: American Meteorological Society Section: Journal of the Atmospheric  
883 Sciences) doi: 10.1175/1520-0469(1993)050<1819:OTRWSA>2.0.CO;2
- 884 Rasch, P. J., Crutzen, P. J., & Coleman, D. B. (2008). Exploring the geoengineering of  
885 climate using stratospheric sulfate aerosols: The role of particle size. *Geophysical*  
886 *Research Letters*, *35*(2). Retrieved 2023-04-19, from  
887 <https://onlinelibrary.wiley.com/doi/abs/10.1029/2007GL032179> (eprint:  
888 <https://onlinelibrary.wiley.com/doi/pdf/10.1029/2007GL032179>) doi:  
889 10.1029/2007GL032179
- 890 Rasmussen, E. N., & Blanchard, D. O. (1998, December). A Baseline Climatology of  
891 Sounding-Derived Supercell and Tornado Forecast Parameters. *Weather and*  
892 *Forecasting*, *13*(4), 1148–1164. Retrieved 2023-01-17, from  
893 [https://journals.ametsoc.org/view/journals/wefo/13/4/  
894 1520-0434\\_1998\\_013\\_1148\\_abcosd\\_2\\_0\\_co\\_2.xml](https://journals.ametsoc.org/view/journals/wefo/13/4/1520-0434_1998_013_1148_abcosd_2_0_co_2.xml) (Publisher: American  
895 Meteorological Society Section: Weather and Forecasting) doi:  
896 10.1175/1520-0434(1998)013<1148:ABCOSD>2.0.CO;2
- 897 Rasmussen, K. L., Prein, A. F., Rasmussen, R. M., Ikeda, K., & Liu, C. (2017, July).  
898 Changes in the convective population and thermodynamic environments in

- 899 convection-permitting regional climate simulations over the United States. *Climate*  
 900 *Dynamics*, 55(1), 383–408. Retrieved 2022-05-12, from  
 901 <https://doi.org/10.1007/s00382-017-4000-7> doi: 10.1007/s00382-017-4000-7
- 902 Riahi, K., van Vuuren, D. P., Kriegler, E., Edmonds, J., O'Neill, B. C., Fujimori, S., ...  
 903 Tavoni, M. (2017, January). The Shared Socioeconomic Pathways and their energy,  
 904 land use, and greenhouse gas emissions implications: An overview. *Global*  
 905 *Environmental Change*, 42, 153–168. Retrieved 2023-01-23, from  
 906 <https://www.sciencedirect.com/science/article/pii/S0959378016300681>  
 907 doi: 10.1016/j.gloenvcha.2016.05.009
- 908 Richter. (2022a). *Assessing Responses and Impacts of Solar climate intervention on the*  
 909 *Earth system with stratospheric aerosol injection simulations (ARISE-SAI-1.5)*.  
 910 UCAR/NCAR - CISL - CDP. Retrieved 2023-07-14, from  
 911 [https://www.earthsystemgrid.org/dataset/id/](https://www.earthsystemgrid.org/dataset/id/29c8320f-c525-4cd2-8014-361ecec3907.html)  
 912 [29c8320f-c525-4cd2-8014-361ecec3907.html](https://www.earthsystemgrid.org/dataset/id/29c8320f-c525-4cd2-8014-361ecec3907.html) doi: 10.5065/9KCN-9Y79
- 913 Richter. (2022b). *CESM2-WACCM-SSP245 simulations*. UCAR/NCAR - CISL - CDP.  
 914 Retrieved 2023-07-14, from [https://www.earthsystemgrid.org/dataset/](https://www.earthsystemgrid.org/dataset/ucar.cgd.cesm2.waccm6.ssp245.html)  
 915 [ucar.cgd.cesm2.waccm6.ssp245.html](https://www.earthsystemgrid.org/dataset/ucar.cgd.cesm2.waccm6.ssp245.html) doi: 10.26024/0CS0-EV98
- 916 Richter, J., Visioni, D., MacMartin, D., Bailey, D., Rosenbloom, N., Lee, W., ...  
 917 Lamarque, J.-F. (2022, April). *Assessing Responses and Impacts of Solar climate*  
 918 *intervention on the Earth system with stratospheric aerosol injection (ARISE-SAI)*  
 919 (preprint). Climate and Earth system modeling. Retrieved 2022-10-31, from  
 920 <https://egusphere.copernicus.org/preprints/2022/egusphere-2022-125/>  
 921 doi: 10.5194/egusphere-2022-125
- 922 Rodgers, K. B., Lee, S.-S., Rosenbloom, N., Timmermann, A., Danabasoglu, G., Deser,  
 923 C., ... Yeager, S. G. (2021, December). Ubiquity of human-induced changes in  
 924 climate variability. *Earth System Dynamics*, 12(4), 1393–1411. Retrieved  
 925 2022-05-12, from <https://esd.copernicus.org/articles/12/1393/2021/> doi:  
 926 10.5194/esd-12-1393-2021
- 927 Sardeshmukh, P. D., & Hoskins, B. J. (1988, April). The Generation of Global Rotational  
 928 Flow by Steady Idealized Tropical Divergence. *Journal of the Atmospheric Sciences*,  
 929 45(7), 1228–1251. Retrieved 2022-09-19, from [https://journals.ametsoc.org/](https://journals.ametsoc.org/view/journals/atsc/45/7/1520-0469_1988_045_1228_tgogrf_2_0_co_2.xml)  
 930 [view/journals/atsc/45/7/1520-0469\\_1988\\_045\\_1228\\_tgogrf\\_2\\_0\\_co\\_2.xml](https://journals.ametsoc.org/view/journals/atsc/45/7/1520-0469_1988_045_1228_tgogrf_2_0_co_2.xml)  
 931 (Publisher: American Meteorological Society Section: Journal of the Atmospheric

- 932 Sciences) doi: 10.1175/1520-0469(1988)045<1228:TGOGRF>2.0.CO;2
- 933 Seeley, J. T., & Romps, D. M. (2015, March). The Effect of Global Warming on Severe  
934 Thunderstorms in the United States. *Journal of Climate*, 28(6), 2443–2458.  
935 Retrieved 2023-03-30, from [https://journals.ametsoc.org/view/journals/  
936 clim/28/6/jcli-d-14-00382.1.xml](https://journals.ametsoc.org/view/journals/clim/28/6/jcli-d-14-00382.1.xml) (Publisher: American Meteorological Society  
937 Section: Journal of Climate) doi: 10.1175/JCLI-D-14-00382.1
- 938 Sellar, A. A., Jones, C. G., Mulcahy, J. P., Tang, Y., Yool, A., Wiltshire, A., ...  
939 Zerroukat, M. (2019). UKESM1: Description and Evaluation of the U.K. Earth  
940 System Model. *Journal of Advances in Modeling Earth Systems*, 11(12), 4513–4558.  
941 Retrieved 2023-03-24, from  
942 <https://onlinelibrary.wiley.com/doi/abs/10.1029/2019MS001739> (\_eprint:  
943 <https://onlinelibrary.wiley.com/doi/pdf/10.1029/2019MS001739>) doi:  
944 10.1029/2019MS001739
- 945 Simpson, I. R., Tilmes, S., Richter, J. H., Kravitz, B., MacMartin, D. G., Mills, M. J., ...  
946 Pendergrass, A. G. (2019). The Regional Hydroclimate Response to Stratospheric  
947 Sulfate Geoengineering and the Role of Stratospheric Heating. *Journal of  
948 Geophysical Research: Atmospheres*, 124(23), 12587–12616. Retrieved 2023-06-20,  
949 from <https://onlinelibrary.wiley.com/doi/abs/10.1029/2019JD031093>  
950 (\_eprint: <https://onlinelibrary.wiley.com/doi/pdf/10.1029/2019JD031093>) doi:  
951 10.1029/2019JD031093
- 952 Smith, W., & Wagner, G. (2018, November). Stratospheric aerosol injection tactics and  
953 costs in the first 15 years of deployment. *Environmental Research Letters*, 13(12),  
954 124001. Retrieved 2023-05-23, from  
955 <https://dx.doi.org/10.1088/1748-9326/aae98d> (Publisher: IOP Publishing)  
956 doi: 10.1088/1748-9326/aae98d
- 957 Stroeve, J. C., Kattsov, V., Barrett, A., Serreze, M., Pavlova, T., Holland, M., & Meier,  
958 W. N. (2012). Trends in Arctic sea ice extent from CMIP5, CMIP3 and  
959 observations. *Geophysical Research Letters*, 39(16). Retrieved 2023-01-20, from  
960 <https://onlinelibrary.wiley.com/doi/abs/10.1029/2012GL052676> (\_eprint:  
961 <https://onlinelibrary.wiley.com/doi/pdf/10.1029/2012GL052676>) doi:  
962 10.1029/2012GL052676
- 963 Strzepek, K., Yohe, G., Neumann, J., & Boehlert, B. (2010, December). Characterizing  
964 changes in drought risk for the United States from climate change. *Environmental*

- 965 *Research Letters*, 5(4), 044012. Retrieved 2023-01-20, from  
 966 <https://dx.doi.org/10.1088/1748-9326/5/4/044012> doi:  
 967 10.1088/1748-9326/5/4/044012
- 968 Taszarek, M., Allen, J. T., Groenemeijer, P., Edwards, R., Brooks, H. E., Chmielewski,  
 969 V., & Enno, S.-E. (2020, December). Severe Convective Storms across Europe and  
 970 the United States. Part I: Climatology of Lightning, Large Hail, Severe Wind, and  
 971 Tornadoes. *Journal of Climate*, 33(23), 10239–10261. Retrieved 2022-10-20, from  
 972 <https://journals.ametsoc.org/view/journals/clim/33/23/jcliD200345.xml>  
 973 (Publisher: American Meteorological Society Section: Journal of Climate) doi:  
 974 10.1175/JCLI-D-20-0345.1
- 975 Thompson, D. B., & Roundy, P. E. (2013, June). The Relationship between the  
 976 Madden–Julian Oscillation and U.S. Violent Tornado Outbreaks in the Spring.  
 977 *Monthly Weather Review*, 141(6), 2087–2095. Retrieved 2023-05-22, from [https://](https://journals.ametsoc.org/view/journals/mwre/141/6/mwr-d-12-00173.1.xml)  
 978 [journals.ametsoc.org/view/journals/mwre/141/6/mwr-d-12-00173.1.xml](https://journals.ametsoc.org/view/journals/mwre/141/6/mwr-d-12-00173.1.xml)  
 979 (Publisher: American Meteorological Society Section: Monthly Weather Review)  
 980 doi: 10.1175/MWR-D-12-00173.1
- 981 Tilmes, S., Richter, J. H., Kravitz, B., MacMartin, D. G., Mills, M. J., Simpson, I. R., ...  
 982 Ghosh, S. (2018, November). CESM1(WACCM) Stratospheric Aerosol  
 983 Geoengineering Large Ensemble Project. *Bulletin of the American Meteorological*  
 984 *Society*, 99(11), 2361–2371. Retrieved 2022-06-07, from [https://](https://journals.ametsoc.org/view/journals/bams/99/11/bams-d-17-0267.1.xml)  
 985 [journals.ametsoc.org/view/journals/bams/99/11/bams-d-17-0267.1.xml](https://journals.ametsoc.org/view/journals/bams/99/11/bams-d-17-0267.1.xml)  
 986 (Publisher: American Meteorological Society Section: Bulletin of the American  
 987 Meteorological Society) doi: 10.1175/BAMS-D-17-0267.1
- 988 Tippett, M. K., Allen, J. T., Gensini, V. A., & Brooks, H. E. (2015, June). Climate and  
 989 Hazardous Convective Weather. *Current Climate Change Reports*, 1(2), 60–73.  
 990 Retrieved 2023-01-24, from <https://doi.org/10.1007/s40641-015-0006-6> doi:  
 991 10.1007/s40641-015-0006-6
- 992 Tippett, M. K., Lepore, C., & L’Heureux, M. L. (2022, September). Predictability of a  
 993 tornado environment index from El Niño–Southern Oscillation (ENSO) and the  
 994 Arctic Oscillation. *Weather and Climate Dynamics*, 3(3), 1063–1075. Retrieved  
 995 2023-03-31, from <https://wcd.copernicus.org/articles/3/1063/2022/>  
 996 (Publisher: Copernicus GmbH) doi: 10.5194/wcd-3-1063-2022
- 997 Trapp, R. J., Diffenbaugh, N. S., Brooks, H. E., Baldwin, M. E., Robinson, E. D., & Pal,

- 998 J. S. (2007, December). Changes in severe thunderstorm environment frequency  
999 during the 21st century caused by anthropogenically enhanced global radiative  
1000 forcing. *Proceedings of the National Academy of Sciences*, *104*(50), 19719–19723.  
1001 Retrieved 2022-11-04, from  
1002 <https://www.pnas.org/doi/abs/10.1073/pnas.0705494104> (Publisher:  
1003 Proceedings of the National Academy of Sciences) doi: 10.1073/pnas.0705494104
- 1004 Trapp, R. J., Diffenbaugh, N. S., & Gluhovsky, A. (2009). Transient response of severe  
1005 thunderstorm forcing to elevated greenhouse gas concentrations. *Geophysical*  
1006 *Research Letters*, *36*(1). Retrieved 2023-02-07, from  
1007 <https://onlinelibrary.wiley.com/doi/abs/10.1029/2008GL036203> (eprint:  
1008 <https://onlinelibrary.wiley.com/doi/pdf/10.1029/2008GL036203>) doi:  
1009 10.1029/2008GL036203
- 1010 Trapp, R. J., Hoogewind, K. A., & Lasher-Trapp, S. (2019, September). Future Changes  
1011 in Hail Occurrence in the United States Determined through Convection-Permitting  
1012 Dynamical Downscaling. *Journal of Climate*, *32*(17), 5493–5509. Retrieved  
1013 2023-03-31, from [https://journals.ametsoc.org/view/journals/clim/32/17/](https://journals.ametsoc.org/view/journals/clim/32/17/jcli-d-18-0740.1.xml)  
1014 [jcli-d-18-0740.1.xml](https://journals.ametsoc.org/view/journals/clim/32/17/jcli-d-18-0740.1.xml) (Publisher: American Meteorological Society Section:  
1015 Journal of Climate) doi: 10.1175/JCLI-D-18-0740.1
- 1016 UNEP. (2022, October). Emissions Gap Report 2022: The Closing Window - Climate  
1017 Crisis Calls for Rapid Transformation of Societies. Retrieved 2023-04-19, from  
1018 <https://wedocs.unep.org/xmlui/handle/20.500.11822/40874> (Accepted:  
1019 2022-10-19T13:29:26Z)
- 1020 Visioni, D., Bednarz, E. M., Lee, W. R., Kravitz, B., Jones, A., Haywood, J. M., &  
1021 MacMartin, D. G. (2023, January). Climate response to off-equatorial stratospheric  
1022 sulfur injections in three Earth system models – Part 1: Experimental protocols and  
1023 surface changes. *Atmospheric Chemistry and Physics*, *23*(1), 663–685. Retrieved  
1024 2023-02-13, from <https://acp.copernicus.org/articles/23/663/2023/>  
1025 (Publisher: Copernicus GmbH) doi: 10.5194/acp-23-663-2023
- 1026 Visioni, D., MacMartin, D. G., Kravitz, B., Boucher, O., Jones, A., Lurton, T., ...  
1027 Tilmes, S. (2021, July). Identifying the sources of uncertainty in climate model  
1028 simulations of solar radiation modification with the G6sulfur and G6solar  
1029 Geoengineering Model Intercomparison Project (GeoMIP) simulations. *Atmospheric*  
1030 *Chemistry and Physics*, *21*(13), 10039–10063. Retrieved 2023-04-20, from

1031 <https://acp.copernicus.org/articles/21/10039/2021/> (Publisher: Copernicus  
1032 GmbH) doi: 10.5194/acp-21-10039-2021

1033 Weisman, M. L., & Klemp, J. B. (1982, June). The Dependence of Numerically Simulated  
1034 Convective Storms on Vertical Wind Shear and Buoyancy. *Monthly Weather*  
1035 *Review*, 110(6), 504–520. Retrieved 2023-01-24, from  
1036 [https://journals.ametsoc.org/view/journals/mwre/110/6/  
1037 1520-0493\\_1982\\_110\\_0504\\_tdonsc\\_2\\_0\\_co\\_2.xml](https://journals.ametsoc.org/view/journals/mwre/110/6/1520-0493_1982_110_0504_tdonsc_2_0_co_2.xml) (Publisher: American  
1038 Meteorological Society Section: Monthly Weather Review) doi:  
1039 10.1175/1520-0493(1982)110<0504:TDONSC>2.0.CO;2

1040 Wilks, D. S. (2016, December). “The Stippling Shows Statistically Significant Grid  
1041 Points”: How Research Results are Routinely Overstated and Overinterpreted, and  
1042 What to Do about It. *Bulletin of the American Meteorological Society*, 97(12),  
1043 2263–2273. Retrieved 2023-06-20, from [https://journals.ametsoc.org/view/  
1044 journals/bams/97/12/bams-d-15-00267.1.xml](https://journals.ametsoc.org/view/journals/bams/97/12/bams-d-15-00267.1.xml) (Publisher: American  
1045 Meteorological Society Section: Bulletin of the American Meteorological Society)  
1046 doi: 10.1175/BAMS-D-15-00267.1

1047 Zarnetske, P. L., Gurevitch, J., Franklin, J., Groffman, P. M., Harrison, C. S., Hellmann,  
1048 J. J., . . . Yang, C.-E. (2021, April). Potential ecological impacts of climate  
1049 intervention by reflecting sunlight to cool Earth. *Proceedings of the National*  
1050 *Academy of Sciences*, 118(15), e1921854118. Retrieved 2023-04-19, from  
1051 <https://www.pnas.org/doi/full/10.1073/pnas.1921854118> (Publisher:  
1052 Proceedings of the National Academy of Sciences) doi: 10.1073/pnas.1921854118